PHASE TRANSITIONS IN ONE-DIMESIONAL HOLSTEIN-HUBBARD CHAIN AND RING

A thesis submitted in partial fulfillment of the award of the degree of

DOCTOR OF PHILOSOPHY

In

PHYSICS

Ву

Chintapanti Uma Lavanya

(Reg no: 12PHPH08)

Supervisor: Prof. Ashok Chatterjee



School of Physics University of Hyderabad Hyderabad 500 046 India

November 2021

DECLARATION

I, Chintapanti Uma Lavanya, hereby declare that the work presented in this thesis entitled Phase Transitions in One-Dimensional Holstein Hubbard Chain and Ring has been carried out by me in the School of Physics, University of Hyderabad, India, under the supervision of Prof. Ashok Chatterjee as per the Ph.D. ordinances of the University. I declare, to the best of my knowledge, that no part of this thesis has been submitted for the award of a research degree of any other University. I hereby agree that my thesis can be deposited in Shodhganga/INFLIBNET.

A report on plagiarism statistics from the University librarian is enclosed.

Place: Hyderabad

Date: 17/11/2021

(Chintapanti Uma Lavanya) Reg. No. 12PHPH08

Chumalevanya



CERTIFICATE

This is to certify that the thesis entitled, "Phase transitions in one-dimensional Holstein Hubbard chain and ring", being submitted to the University of Hyderabad by **Chintapanti Uma Lavanya** bearing Reg. No. 12PHPH08 in partial fulfillment of the requirements for the award of the degree of Doctor of Philosophy in Physics, is a record of bonafide work carried out by her under my supervision and is free of plagiarism.

This matter embodied in this report has not been submitted to any other University or Institution for the award of any degree or diploma.

Further, the student has the following publications (1-2) in international peer reviewed journals and conference proceedings (3-4) before the submission of the thesis for adjudication.

- Ch. Uma Lavanya, I.V. Sankar and Ashok Chatterjee, Metallicity in a Holstein-Hubbard Chain at half filling with Gaussian Anharmonicity, *Scientific Reports* 7 3774 (2017). (Chapter 2 is written based on this Paper).
- 2. **Ch. Uma Lavanya** and Ashok Chatterjee, Persistent and Spin Currents in the 1D Holstein-Hubbard ring at half filling and at away from half-filling by Bethe-ansatz approach, Physica E 126 114500 (2021). **(Chapter 3 is written based on this Paper).**
- 3. **Ch. Uma Lavanya** and Ashok Chatterjee, The Holstein-Hubbard Model with Gaussian Anharmonicity in one-Dimension at Half-filling, AIP Conference Proceedings 1728 020477 (2016).

 Ch. Uma Lavanya and Ashok Chatterjee, Metallicity of the anharmonic Holstein-Hubbard Model in the adiabatic regime, AIP Conference Proceedings 1942 090003 (2018).

Further, the student has passed the following courses towards the fulfillment of course-work required for Ph. D.

S. No	Course Code	Name of the Course	Credits	Pass/Fail
1	PY801	Advanced Quantum Mechanics	4	Pass
2	PY803	Advanced Statistical Mechanics	4	Pass
3	PY804	Advanced Electromagnetic Theory	4	Pass
4	PY821	Research Methodology 4		Pass

Prof. Ashok Chatterjee

Prof. ASHOK CHATTERJEE SCHOOL OF PHYSICS UNIVERSITY OF HYDERABAD HYDERABAD - 500 046, INDIA

Thesis Supervisor

University of Hyderabad

Dean

Place: Hyderabad

Date: 17 | 11 | 2021

School of Physics

University of Hyderabad संकाय अध्यक्ष / Dean

भौतिकी संकाय / School of Physics

हैदराबाद विश्वविद्यालय UNIVERSITY OF HYDERABAD

हैदरावाद / HYDERABAD-500 046. भारत / INDIA.

Dedicated

To my Parents

Chintapanti Padma & Subbaiah

And

To the Humanist, rationalist, and human rights activist

Mr. Babu Gogineni

Preface

In this thesis we shall present our works on the nature of phase transitions in a dimensional Holstein-Hubbard chain and the persistent current in a Holstein-Hubbard ring. These works fall under the broad area of strongly correlated systems in theoretical condensed matter physics. Usually the strongly correlated electron systems are narrow-band systems the study of which is based on the tight-binding model. In the absence of electron-electron (*e-p*) and electron-phonon (*e-p*) interactions, the tight binding model is simple. It contains only a hopping term with an overlap integral t, called the hopping parameter which essentially measures the kinetic energy of the electrons. This model is exactly soluble.

Though this model has worked well, it fails to explain why some materials like transition metal oxides are insulators which are now known as Mott insulators. Mott explained that when the onsite e-e correlation is much stronger than the hopping kinetic energy, electrons get localized at their respective sites leading to an antiferromagnetic insulating state. A convincing theory for such materials was developed by Hubbard using a model known as the Mott-Hubbard model or simply the Hubbard model which has in addition to the nearest neighbour (NN) hopping term, an onsite correlation term which contains a Coulomb repulsive interaction with a parameter U that gives the strength of the interaction.

One can also have a system of electrons interacting with phonons with ignorable electron-electron interaction in a narrow-band material. Such a material can have polarons and bipolarons as quasiparticles. This localized electron-phonon (e-p) system can be described by the celebrated Holstein model which has a hopping term and an onsite e-p interaction term. One can of course have a more general system having both *e-e* and *e-p* interactions. This system can have interesting phase diagrams because of the interplay between the e-e and e-p interactions. A suitable model for such a system is the Holstein-Hubbard (HH) model which is a combination of the Hubbard model and the Holstein model. The tight-binding hopping term of the HH model tries to delocalize the electrons, whereas the onsite e-e interaction term induces electron localization leading to the formation of local moments and the onsite e-p interaction creates lattice distortions and hence a polarization potential which can localize at a lattice site one or two electrons depending on the relative strengths of the e-e and e-p interactions. Thus, the HH model can explain a variety of phenomena like the formation of polarons and bipolarons, self-trapping transition, metal-insulator transitions of Mott or Peierls superconductivity, high-temperature colossal magnetoresistance and so on.

It is well known that the pairing mechanism for the high-temperature superconductivity (HTCS) is still not yet clear. A group of researchers have advocated the electronic mechanism as the cause of superconductivity in the cuprates. However, quite a few researchers have also suggested the phonon mechanism. Since high-T_c materials like cuprates are strongly correlated narrow band systems, the HH model should be the suitable model to investigate the HTSC in cuprates. Unfortunately, however, the explanation of superconductivity using the

HH model runs into a serious difficulty. To understand this, one has to look into the nature of the ground states provided by the HH model. The HH system can have different quantum phases. When the e-p interaction is small, the ground state of the HH system is a spin-density wave (SDW) state and when the e-p interaction is strong, the ground state of the system is a charge density wave (CDW) state. This is not an encouraging scenario from the point of view of superconductivity because to achieve high transition temperature one needs to have strong e-p interaction, while the strong e-p interaction leads the system into a CDW insulator. Thus, superconductivity looks impossible in the HH model. Of course, one may be curious to study the transition region. In their report, Hirsch and Fradkin performed a Monte-Carlo study of the HH model and showed that the transition from SDW phase to CDW phase is direct so that there is no metallic phase in the HH model at all.

Takada and Chatterjee in 2003 took up the 1D half-filled HH model for a more critical investigation and studied the SDW-CDW transition in this system using a variational method coupled with the Bethe ansatz. Their analysis shows that there exists an intervening metallic phase at the crossover of the SDW-CDW transition. This result was obtained with the harmonic approximation for the lattice vibrations which implies that a phonon has an infinite life time. So to deal with the real materials we need to consider the finite lifetime effect for the phonons. This can be done by considering anharmonic phonons. In 2004, Chatterjee and Takada performed a calculation including cubic and quartic anharmonicities in the lattice

potential. Interestingly, their results show that the width of the metallic phase widens in the presence of anharmonic phonons. In the present thesis, we will present an improved variational calculation to unravel the nature of the phase transition in the HH model with a Gaussian phonon anharmonicity. We will also present a calculation of the persistent current in a HH quantum ring.

The organization of the thesis is as follows. In Chapter 1, we introduce the subject of the thesis in general and discuss the motivation for carrying out this work. We first describe the Tight-Binding model and then introduce electron correlation and the Hubbard Model. Thereafter we touch upon the concept of phonons and present the Holstein model. In this context we discuss polarons and bipolarons. Next, we present a brief introduction to the HH model and discuss the SDW and CDW phases. Finally, we introduce the concept of persistent current.

In Chapter 2, we consider the one-dimensional HH model with Gaussian phonon anharmonicity to study the possible phase transitions in the ground state. Here we consider a better variational phonon state than what was considered earlier by Chatterjee and Takada in 2003 and obtain an effective Hubbard model which we solve exactly using the Bethe ansatz technique to obtain the GS energy. Consequently, we calculate the local spin moment, the double occupancy, entanglement entropy and consider the Mott criterion for all band fillings. Our results show the emergence of a metallic phase flanked by SDW and CDW insulating ground states confirming the predictions of Chatterjee and Takada. We also show that

the Gaussian anharmonicity increases the width of the metallic phase.

In Chapter 3, we are interested in studying the effect of e-p interaction on the persistent current in a quantum ring threaded by a magnetic flux through the center of the ring. To study this problem, we use the extended HH model in which we consider onsite and nearest-neighbour e-p interactions. We eliminate the phonon degrees of freedom using a unitary transformation followed by a zero-phonon averaging. This leads to an effective Hubbard model which we solve exactly by the Bethe ansatz technique and also approximately using the Hartree-Fock approximation to obtain the ground state energy. We study the characteristics of the persistent charge and spin currents, Drude weight and effect of e-e and e-p interactions on them. We have also studied the Mott criteria, local spin moment, double occupancy and entanglement entropy of the system to study the phase transitions of the system. The phase diagram shows the existence of an intermediate metallic phase in the ground state when the e-e and e-p interactions are comparable to each other. Furthermore, we show that the width of the metallic phase increases as the electron density decreases from the half-filling.

Finally in Chapter 4, we briefly summarize our results and make a few comments on our findings.

It is a real delight to acknowledge those who have supported and encouraged me a lot to finish my Ph.D. Firstly, I would like to express my deepest and sincere gratitude to my mentor, guru, supervisor and well-wisher, Prof. Ashok Chatterjee, for giving me the opportunity to join his research group. I would like to specially thank him for his teaching and inspiring attitude that enabled me to pursue my Ph.D. in the exciting field of Theoretical Condensed Matter Physics. I would also like to thank him for his guidance and motivation. It is an honor and privilege for me to work under his supervision. I am very much delighted with our countless discussions particularly grateful for all the advice I received from him. I would like to specially thank Dr. Soma Mukhopadhyay for treating me as their family member during my stay on the campus.

Besides my supervisor, I would like to express my deepest gratitude to my doctoral review committee members: **Prof. S. Srinath** and **Prof. S.V.S.**Nageswara Rao not only for their valuable suggestions and insightful comments on my research during the doctoral committee meetings but also strong support that they provided after I became a better half of Dr. B. Ravi Kumar. In the same regard, I am greatly honored to express my thanks to Prof. S. N. Kaul and Manju madam. It gives me an immense pleasure to express my sincere gratitude to present Dean of School of Physics, Prof. Ashok Chatterjee and former Deans, Prof. Sheshu Bhai, Prof. Bindu A

Bamba, Prof. R. Singh, Prof. S. Chaturvedi, Prof. S.P. Tewari and Prof. C. Bansal for providing needful facilities when required.

I am grateful to Prof. Ashok Kapoor, Prof. K. P. N. Moorthy, Prof. P. K. Suresh, Prof. V. S. S. Sasthry, and Prof. Surajith Dhara for giving me valuable suggestions whenever I approached them.

I would like to pay special thanks to Mr. T. Abraham sir, Gaddam Srinivas sir, Mrs. Deepika, Mrs. Shailaja, Mr. Prasad, Mr. Sudharshan sir, Mr. Somu and all other non-teaching staff of School of Physics for their help and support.

I would like to pay special thanks to Dr. I.V. Shankar, Dr. B. Aalu Naik, Dr. P.J. Monisha, Dr. D. Sanjeev Kumar and Dr. Ch. Narasimha Raju for their useful scientific discussions to make my understanding of Physics a better way. For this, I treat them as my gurus since then.

On the same note, I must thank my colleague Dr. Luhluh Jahan K for her amiable personality, caring and support throughout my Ph.D. She is more than a friend to me. I enjoyed her company when we worked together. She is great companion to me. Special thanks to Ms. Manasa Kalla for her timely help. I am grateful to my other lab mates: Mr. Rajendar kumar Bhuyan (late), Mr. Zahid Malik, Mr. Hemanth Kumar Sharma, Ms. Pooja Saini, Mr. Kunthal Bhattacharya and Ms. Debika Debnath. I would also like to express

my special thanks to Dr. Athahar Parveen for her constant moral support and scientific discussions from the time we met together.

I am very grateful to my seniors and friends: Dr. K. Suman Kalyan, Dr. Iyyappan, Mr. M. Yadaiah. Dr. S. Pavan Kumar Naik and his cute family: Sandhya Rani, little angel Aira, Dr. E. Sivanagi Reddy, Sajala and little Nikhil, Dr. T. Anil Kumar and Jayasree, M. Uma Sankar (late) and Poornima, Dr. M. Pavan Venu Prakash, Dr. Yugandhar Bitla, Dr. Suresh Pittala, Dr. Pd Sankar, Dr. A. Ramesh, Dr. Raju Botta, Dr. Shiva N Chari, Dr. Shaik Ahmed, Dr. Anantha Ramulu, Dr. Narasimhappa, Dr. Anusha Shylaja Thilakan, Dr. Babu Rao Gona, Dr. Hyma Salava (Plant Science), Dr. Gatla Shiva (Oceonology), Mrs. Prasanna Kumari, Dr. E. Ramya, Dr. M. Dhanunjay, Dr. Rashmitha Sahoo, Mr. Nagaraj (Anthropology), Dr. Srinivas (SEST), Dr. Pagidi Srinivas, Dr. M. Sandeep, Dr. Santhanu Padi, Dr. Merugu Ramchandhar, Dr. Binoy Krishna Hazra, Ms. Leela shree, Mr. Avishek Das, Mrs. B. Praneetha, Mr. Najir Islam, Mrs. KM Ashwathi, Mrs. P. Ramya (History), Mrs. Renuka Pullimavidi, Ms. Amala Rao (Computer Science), Ms. Mounika. I thank my dearest friend, Dr. M. Ramanatha for his caring and support.

I thank my friends during my M.Sc. course, Mr. Sandeep, Mr. Prathap, Mr. Ramesh, Dr. Kalam, Dr. Azmath, Ms. Shobha rani, Ms. Sandhya Rani, Dr. Koteswara Rao, Dr. Linga Moorthi, Ms. Sona Chandran, Ms. Jinisha, Dr. Anjana, Dr. Narayan

Behera, Dr. Shravan Kumar Appani, Mr. Satheesh, Mr. Sujith, Mr. Mentose for sharing memorable moments with me.

The time in the Hyderabad has been great. I will always remember it as a rewarding life experience. Thanks to everyone who made my stay on the campus so enjoyable and memorable.

I am honored to express my gratitude to B.Sc. Lecturers from S.P.W.D. College, Tirupati. Mrs. Jayashree, Mrs. Uma Devi, Mrs. Uma Maheswari, Mrs. Praveena, Mrs. Bala Krishna Priya, Mrs. Dhana Lakshmi, Mrs. Sandhya Rani, Mrs. Bharathi, Mrs. Kavitha, Mrs. Jashintha, and friends Mrs. Sravanthi Reddy, Mrs. Aparna Reddy, Mrs. Sathya, Mrs. Madhavi, Mrs. Guramma, Mrs. Rukmini, Mrs. Vaishnavi, Mrs. Savithri, Mrs. Vani, Mrs. Shiva Kumari.

I thank DIET-Pallepadu friends and the present government school teachers Mr. L. Subrahmanyam, Mrs. N. Sreelatha, Mrs. Vineela and many others.

I would like to thank my college teachers from Rao Academy. **Mr. G. Mallikharjuna Rao** is my English teacher who introduced me the proper way of learning. **Mr. K. Kondala Rao** is my Maths teacher. I have to thank both of them for their constant love, caring, encouragement and support without whom I have not been this far. I would also thank Mr. Nageswara Rao, Mr. Venkata Ramanaiah, Mr. Sreenu

Anna, Mrs. Padma, Mr. Venkateswarlu, Mr. Jagan, who inspired me through their teachings and constant encouragement. I also thank my college friends Mrs. Sumathi, Mrs. Haritha, Mrs. Fahmeena, Mrs. Mobeena, Mr. Srinivasula Reddy (late). The days of my intermediate education were enjoyable and memorable.

I am eternallly grateful to my high school teachers from G.H.S. Pallepadu, Nellore Mr. A. Kamaiah, Mr. K. Venkateswarlu, Mrs. Annapoorna, Mr. Srihari, Mr. Milton, Mr. Basha, Mrs. Susheela.

I owe huge gratitude to my Violin teachers Mr. Kolanka Sai, Mr. Kolanka Anil and Prof. Kavi Narayana Murthy for their marvellous way of teaching music.

I would like to greatly acknowledge the Council of Scientific & Industrial Research (CSIR), India for providing financial support with CSIR-JRF and SRF.

I am lucky have my *Chinna Pedananna* Purini Sree Ramulu, my *Pedda pedamma* Mrs. Auta Raja Rajeswaramma in my life. Their help is countless. I thank Dasari Kavitha and her family for helping me. A special mention of my lovable brother **Ch. Naveen Kumar** for his love, caring and support. I am grateful to my dearest cousin **Mr. Auta Shiva Sankar** who has been a role model for my entire life. He enlightened me with his vision.

Finally, I wish to thank my beloved parents for their caring, love and encouragement, without whom I would never have completed my Ph.D. I am fortunate to have parents like that who always try to give their best to help whatever way they can and extremely helpful for me. A mere thanks may not be enough to show my gratitude but except saying that "I will be always grateful to them".

I would like to thank my caring husband **Dr. B Ravi Kumar** for his constant help and support. I am very much thankful to have a baby boy **Ishan Karthi.** We call him Magnu. He is such a lovely baby to make my life happy like anything.

I also would like to thank **Mr. Babu Gogineni** for his views towards the human life. He is one of the role models I have in my life.

CONTENTS

Ch	apter	1: Introduction	1
1.1	Energy	Bands	3
1.2	Tight B	inding Model	4
1.3	The Hu	bbard Model	8
1.4	Phonor	าร	10
1.5	Polaror	ns	12
1.6	Holstei	n Model	13
1.7	Holstei	n-Hubbard Model (HHM)	15
	(i)	Spin Density Wave (SDW)	17
	(ii)	Charge Density Wave (CDW)	19
1.8	Persist	ent Currents	22
1.9	Organiz	zation of Thesis	24
Ref	erences		25

Chapt	ter 2: Metallicity in Holste	in-Hubbard
	chain at half-filling with	
	anharmonicity	29
2.1	Introduction	29
2.2	The Model	33
2.3	Formulation	34
	2.3.1 GS Energy	34
	2.3.2. Local Spin Moment (LSP)	45
	2.3.3. Entanglement Entropy (EE)	46
2.4. N	umerical Results and Discussion	47
2.5. Co	nclusion	68
Refere	nces	68

Holst	ein-Hน	Persistent	ng by	Bethe-ar	nsatz
3.1	Introd	uction			73
3.2	Hamilt	onian and the	Model		75
3.3	Formu	lation			76
	3.3.1	GS Energy			76
	3.3.2	Persistent	Charge	Current	and
		Persistent Sp	oin Current		81
3.4	Results	s and Discussion	on		82
	3.4.1	GS Energy			82
	3.4.2	Persistent C	harge Curi	rent (PCC)	85
		(a) Flux depe	endence of	F PCC	85
		(b) PCC and	Coulomb C	Correlation	88
		(c) PCC and e	e-p interact	tions	93

	(d) PCC and Phase transitions97
	(e) Size dependence of PCC106
3.4.3	Persistent Spin Current (PSC)109
	(a) Flux-dependence of PSC109
	(b) PSC and Coulomb Correlation110
	(c) PSC and <i>e-p</i> interactions112
	(d) Size dependence of PCC113
3.5. Summary	and Conclusion114
References	116
Chapter 4: S	Summary and Conclusions119
References	123

Chapter 1

Introduction

Materials play a vital role in the development of human civilization. Since ancient times, humans have been trying to make and use materials in ingenious ways to suit their purposes. Human thinking has made the impossible possible. For example, before the modern era of scientific development, one-dimensional systems (1D) were almost non-physical. But now one-dimensional quantum chains are made in the laboratory and have very interesting properties. The classification of materials available in nature has been well developed. Regardless of the type of bond, any solid can be considered a combination of electrons and nuclei. Despite the considerable progress made in the materials, we still need more advanced research methods to raise the quality of human life.

For scientists, defining a theoretical model to classify materials such as metals and insulators has always been the most difficult challenge and must be consistent with the experimental results. In course of time, several materials ranging from simple elements to ceramic materials, transition metal oxides, charge transfer oxides and other composite materials. Finding the energy of any material is an important key to meeting the material requirements. In the field of Condensed Matter Physics (CMP), we often focus on the ground state energy (GS) of the system and the factors that affect GS energy. Materials consist of electrons and ions and the arrangement, structure and rhythm of these particles contribute to the GS energy of the material. Both structure and properties depend on the configuration of the electrons and ions. In general, electrons contain a sizable part of energy in any system. It is believed that the metallic properties of the system depend only on the electronic properties. The energy of a system can be found in several ways. Schrödinger came up with his equation using wave mechanics to treat a system quantum mechanically for finding the GS energy. This equation is widely known and well celebrated in quantum mechanics. However, the Schrödinger equation could not be solved exactly for real systems and therefore approximate methods like the perturbation theory, the variational methods and the exact diagonalization methods were introduced to find the GS energy of a system. Later, these methods turned to be inappropriate in several cases and more advanced methods were suggested. It was discovered that the interactions of electrons with other

electrons, and also with other types of particles like phonons also change the energy of the system. Hence, it is fundamentally relevant to consider electron-electron (e-e) interactions and electron-phonon (e-p) interactions.

In the present thesis, we shall present our works on the GS phase diagram for a one-dimensional Holstein-Hubbard model and the persistent current in a Holstein-Hubbard ring. It will therefore be pertinent to introduce in this introductory chapter some of the basic concepts and the necessary models that are required to build the theory for the investigation for the aforementioned problems.

1.1 Energy Bands

Calculating the electronic band structure of solids is very important to understand various physical properties of solids. Any theory that has been constructed to compute the energy band structure of the system is known as the band theory. The fundamental problem in the band theory is to solve the well-known Schrodinger equation.

$$H\,\psi(r) = E\,\psi(r) \tag{1.1}$$

where, $\psi(r)$ is the wave function of the system Hamiltonian H belonging to the eigenvalue. The

system can be a solid crystal, an amorphous material, a liquid or a gas. Since any material is composed of electrons and nuclei, the Hamiltonian contains the coordinates of both the electrons and ions as well. The Born-Oppenheimer approximation facilitates us to decouple the motion of electrons and ions individually. This approximation is also called the adiabatic approximation.

The free-electron theory, nearly free electron theory and the tight-binding theory are some of the general models of the band theory. The free electron theory works well in the case of ignorable electron-electron interaction and the electrons can be considered completely non-interacting. In nearly free electron theory, the effect of interactions can be incorporated as perturbations. In case of materials in which the electron wave functions on neighbouring atoms overlap very little or the electron wave functions are localized, the free electron model is not a proper model. In this thesis, we will use the tight-binding model and therefore in the following sub-section, we present a discussion on this model.

1.2 Tight Binding Model

The Tight binding model (TBM) provides the basis for developing well appreciated many-body theories, such as the t-J model, Anderson impurity model, the Hubbard model (HM) and the Holstein Model. Slater and Koster [1] were the first to call the TBM as Bloch method, and their work provided the meticulous calculation for framing TBM.

To develop theoretical models, we start with some assumptions. In the free-electron theory, the starting assumption is that the valance electrons are free from the atoms and very much free to move throughout the crystal. Whereas in the case of TBM, we start with an isolated atom to which an electron is tightly bound. Several such atoms come closer to form a crystal. If the lattice constant is such that that the electron wave functions overlap, then an electron can move by hopping from one site to another and system will behave like a metal. If the electron wave functions do not overlap at all, then an electron will find it difficult to hop from one site to the other and in this situation, the system behaves like an insulator. If the lattice constant is reduced so that a small overlapping of electron wave functions occurs, then also the electrons will be able to hop from one site to another and the system will have a narrow band, but still it can behave like a metal. Thus, the tight-binding (TB) model can explain the metal-insulator transition. However, there is a constraint on this hopping. For hopping, the formed bands should be partially filled with the electrons. So we can say that the materials with the partially filled valence bands are supposed to be the

metals and the materials with fully filled or empty filled bands are supposed to be insulators.

The Hamiltonian of the TB model in the second quantized notation is as follows

$$H = -\sum_{\langle ij\rangle} t_{ij} c^{\dagger}_{i\sigma} c_{j\sigma} \qquad (1.2)$$

where the notation $\langle i,j \rangle$ implies that the summation is over nearest neighbours i and j only, t_{ij} is the nearest-neighbour hopping integral given by $t_{ij} \cong \frac{1}{N} \sum_{\langle ij \rangle} \varepsilon_k \, e^{ik.(r_i - r_j)}$, ε_k being the energy of the system, $c_{i\sigma}^{\dagger} \, (c_{j\sigma})$ is the creation (annihilation) operator for the electron at site i (j) with spin σ which can be either up (\uparrow) or down (\downarrow) .

The solution can be found by using the Bloch theorem since the crystal contains a periodic potential. In many systems, t_{ij} would be same for all nearest neighbours and so we can assume: $t_{ij} = t$. The energy dispersion relation of the system is given by

$$\varepsilon_k = -t \sum_{\alpha} \cos(k.\alpha) \tag{1.3}$$

For a 1D chain, there are two nearest neighbour atoms and hence $\alpha = \pm a$ and the energy becomes

$$\varepsilon_k = -2t \cos(ka) \tag{1.4}$$

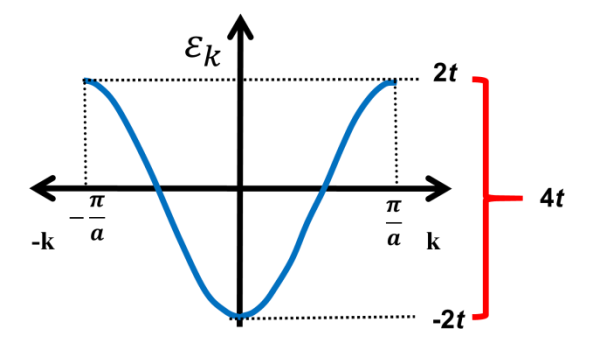


Fig. 1. The energy dispersion relation of TBM for the 1D lattice chain.

According to this model, as the space between the atoms is reduced, the system turns from insulator to metal as the mobility of the electrons increases due to the overlapping of atomic wave functions. Due to the partially filled band, the system is metallic whereas the system behaves as an insulator for a fully filled band. According to this theory, certain substances, such as NiO, CuO₂, V₂O₃, Fe₃O₄ and VnO₂ should behave as metals, but interestingly they behaved as insulators experimentally. Thus, the usual Band theory fails to explain the insulating behaviour of the above materials.

The insulating behavior in these materials was later explained by Mott and Hubbard. It turned out that the insulating behaviour in the afore-mentioned materials is due to the electron-electron Coulomb correlation and these are called Mott insulators. Hubbard proposed a model known as the Hubbard model which gives the proper framework to deal with the correlated systems.

1.3 The Hubbard Model

The Hubbard Model is described by the Hamiltonian

$$H = \sum_{i\sigma} t_0 n_{i\sigma} - t \sum_{\langle ij \rangle \sigma} c_{i\sigma}^{\dagger} c_{j\sigma} + U \sum_{i} n_{i\uparrow} n_{i\downarrow} \quad (1.5)$$

Here the first term is the site energy and the second term is usual tight binding hopping term, t being the hopping amplitude and it represents the kinetic energy. The third term refers to the onsite e-e Coulomb interaction, U giving the on-site Coulomb correlation energy. This model allows the hopping of electrons from one site to another and also allows the electrons to be localized at the atomic sites. So both possibilities are taken care of in this model. This Hamiltonian is meant for the on-site electrons only. When the correlations of inter-site electrons are incorporated, the

resulting model is known as the extended Hubbard-Model.

The Hubbard Model has two limits: (i) $U \to 0$, and (ii) $t \to 0$. In the former, which is known as the band limit, the hopping term solely contributes to the GS energy of the system. This is nothing but the tight-binding Hamiltonian. Here, the Bloch wave functions are the eigenfunctions of the Hamiltonian. In the second limit which is known as the atomic limit, the interaction term (U) of the two particles contributes to the system's GS energy. The Hubbard Model admits exact solutions in both these limits. But, if we combine both the t and U terms together, it is difficult to solve the Hubbard model in general.

Lieb and Wu [2] solved the Hubbard model exactly in one dimension using the Bethe ansatz technique and solving the Fredholm integral equations in the thermodynamic limit i.e., for an infinite chain. This was for the half-filled case. Later Shiba and Pincus [3] solved the same problem for away from half filling. So far it has not been possible to solve the Hubbard model in higher dimensions. However, various methods have been used to obtain approximate solutions of the Hubbard model in higher dimensions.

It was explained by Mott [4] and Hubbard [5] that due to the presence of *e-e* interaction in the Hubbard Model, the energy bands undergo a splitting into two separate sub-bands for each set of spin-up and spin-

down electrons. The lower sub-band consists of the spin-up electrons whereas the upper sub-band consists of the spin-down electrons. The gap between these sub-bands is equal to the onsite Coulomb correlation strength U. For U > t, the Fermi level lies in between the two aforementioned sub-bands leading to an insulating state which is the Mott insulating state.

Over a period of time, the HM has evolved as a well-celebrated model that looks simple but deals with several beautiful phenomena in CMP. In fact, it has emerged as an important model to deal with a subbranch of CMP called the strongly correlated systems. It can give rise to several interesting ground states like magnetic order or superconducting order. It can also predict some interesting quantum phase transitions.

1.4 Phonons

The ions or atoms are considered to be at rest at their corresponding equilibrium positions when the structural and cohesive properties of solids are investigated. This is a reasonably good assumption to study their structural as well as binding properties. However, for some important properties such as thermodynamic properties, this assumption is not sufficient and hence, the dynamics of the lattice must be taken into account. In reality, at finite temperatures, the ions or atoms in solids do not stick to their

equilibrium positions but as a matter of fact, they vibrate or move back and forth continuously with respect to their equilibrium positions. This sort of oscillations is called lattice vibrations. These lattice vibrations are quantized in the quantum mechanical treatment. The quanta of the lattice vibrations are called phonons. In this thesis, we consider harmonic approximation to deal with the phonons.

Phonons can affect the resistivity of metals by interacting with electrons. The interaction of phonons with conducting electrons can also change the ground Polaronic state of the system. effects and Superconductivity are the best examples of this. The phonons are also responsible for the Peierls instability in some of the 1D systems. The phonons can be treated both classically and quantum mechanically. In this thesis, we are interested in quantum behavior of solids and therefore we will consider the quantum mechanical way of dealing the lattice vibrations.

The quantum mechanical Hamiltonian for the interaction of an electron with longitudinal optical phonons in polar materials was first given by Fröhlich in the continuum approximation. This is the celebrated polaron problem. The polaron problem in the tight-binding model was first rigorously discussed by Holstein [6].

1.5 Polarons

Landau [7] was the first who brought the concept of polaron into the limelight with his paper. According to him, a charge carrier either an electron or a hole can distort (or polarize) the medium around it. The induced polarization and the charge carrier together can be considered as a single entity which is called a polaron [8]. Since the polarization field is made up of phonons, it can be considered as a cloud of phonons

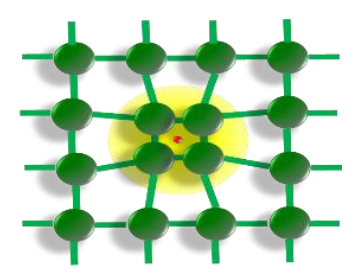


Fig. 2. A polaron in a square lattice of atoms. The electron is screened by a cloud of phonons, the lattices are distorted.

surrounding the charge carrier. Later, Landau and Peker [9] calculated the effective mass and the self-energy of polarons. This analysis corresponds to the strong-coupling or the adiabatic regime and the resulting polaron is called as the strong-coupling polaron or the Peker polaron. Later, Fröhlich [10]

came up with a quantum mechanical Hamiltonian to describe a polaron. The Fröhlich Hamiltonian can be used to deal with polaron for the entire range of the coupling constant. In the case when the *e-p* interaction is weak, the distortion in the lattice can occur over a large number of lattice points and the corresponding polaron is termed as a large polaron. In the strong-coupling regime, the lattice distortion is confined essentially within one lattice spacing and then the resulting polaron is known as the small polaron. A weak-coupling large Fröhlich polaron can move almost freely through the solid medium.

The Fröhlich model is based on the continuum approximation and the formulation has been made in the momentum space. Holstein [6] considered the case of charge carriers in the tight-binding model and therefore the polarons conceived by Holstein are associated with lattice sites in real space and the motion of these polarons happens through hopping between lattice sites. Such a polaron is known as the Holstein Polaron.

1.6 Holstein Model

Holstein [6] gave a new formulation for the polaron problem based on the tight-binding model. The Hamiltonian of this model is as follows.

$$H = -t \sum_{\langle ij \rangle \sigma} c_{i\sigma}^{\dagger} c_{j\sigma} + \hbar \omega_0 \sum_{i} b_i^{\dagger} b_i + g \sum_{i\sigma} n_{i\sigma} (b_i^{\dagger} + b_i)$$
 (1.6)

Here the first term represents the tight-binding hopping term where $c_{i\sigma}^{\dagger}(c_{j\sigma})$ is the electron operator that creates (annihilates) an electron with spin σ at site i with . The second term represents the harmonic lattice Hamiltonian, where $b_i^{\dagger}(b_i)$ denotes the phonon operator that creates (annihilates) a phonon of frequency ω_0 at site i. The phonon operators b_i and b_i^{\dagger} satisfy b_i^{\dagger} the commutation relation: $[b_i, b_j^{\dagger}] = \delta_{ij}$. The third term gives the e-p interaction, g being the e-p interaction strength. As mentioned already, Holstein considered the phonon oscillations to be harmonic.

When two polarons interact, they can form a bound pair if the phonon-mediated attractive interaction between the two electrons can overcome their usual Coulomb repulsion. Such a bound pair of two polarons is known as a bipolaron [6]. These bipolarons are bosons and can undergo Bose-Einstein condensation.

1.7 Holstein-Hubbard Model (HHM)

If the *e-e* interactions and the *e-p* interactions are considered together in the tight-binding model, then the model is called as the Holstein Hubbard Model (HHM).

The Hamiltonian of the HH Model is given by

$$H = \sum_{i\sigma} t_0 n_{i\sigma} - t \sum_{\langle ij \rangle \sigma} c_{i\sigma}^{\dagger} c_{j\sigma} + U \sum_{i} n_{i\uparrow} n_{i\downarrow}$$
$$+ \hbar \omega_0 \sum_{i} b_i^{\dagger} b_i + g \sum_{i\sigma} n_{i\sigma} (b_i^{\dagger} + b_i) \quad (1.7)$$

All terms of this Hamiltonian have already been explained in the earlier sections. This Hamiltonian is useful to determine the nature of the interplay between the *e-p* coupling and the electron correlation. Based on the relative strengths of the different coupling parameters, one would expect the HH model to lead to a certain type of ground state.

Fig.3 describes a one-dimensional (1D) linear atomic chain with a hopping term, an e-e interaction term with strength U and an e-p interaction term with strength g. Thus, the HH model can be used to study the properties of the system in Fig.3. The parameter t gives a measure of electron-hopping and thus

describes delocalization of electrons. The Coulomb repulsion (U) opposes double occupancy and leads to the finite local spin moment in the system. The e-p coupling leads to the formation of onsite polarons. If g is sufficiently large as compared to U, there can be double occupancies at the lattice sites.

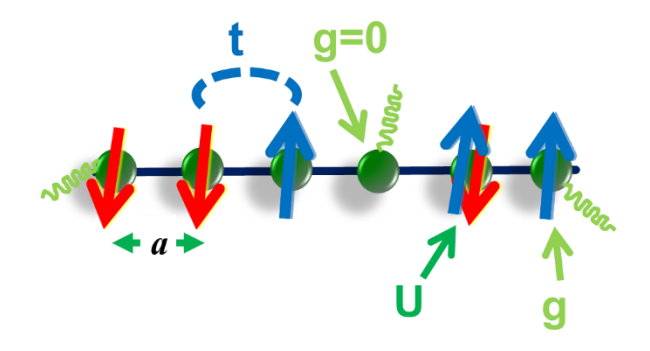


Fig. 3. A One Dimensional (1D) linear atomic chain with hopping term, e-e interaction strength U and the e-p interaction strength g.

The conventional superconductivity is explained by the celebrated BCS mechanism [11]. The pairing mechanism for the high-temperature superconductivity (HTCS) in cuprates has however remained hitherto elusive. A group of researchers have advocated the electronic mechanism as the cause of superconductivity in cuprates. However, quite a few

researchers have also suggested the phonon mechanism. Since high- T_c materials like cuprates are strongly correlated narrow band systems, the HH model should be the suitable model to investigate the HTSC in cuprates. Unfortunately, however, the explanation of superconductivity using the HH model runs into a serious problem. To understand the problem, it will be good to discuss the nature of the ground states provided by the HH model.

The HH system can have different quantum phases. The transitions can also occur within these quantum phases. We describe these ground state phases below for the half-filled HHM case and finite hopping probability t.

(i) Spin Density Wave (SDW)

If the e-e interaction dominates over the e-p interaction (i.e., $U \gg g$), the electrons, because of their strong Coulomb repulsion, cannot hop from one site to another (even though the Pauli principle allows two electrons to be in same quantum state at a particular site with opposite spins). This leads to localization of electrons (or more specifically, polarons) at their respective sites. Since the system is half-filled, i.e., each site is occupied by a single electron; the state looks like an antiferromagnetic state in which alternative sites are

occupied with opposite spins. This is a spin density wave state. As we have already mentioned, in this state,

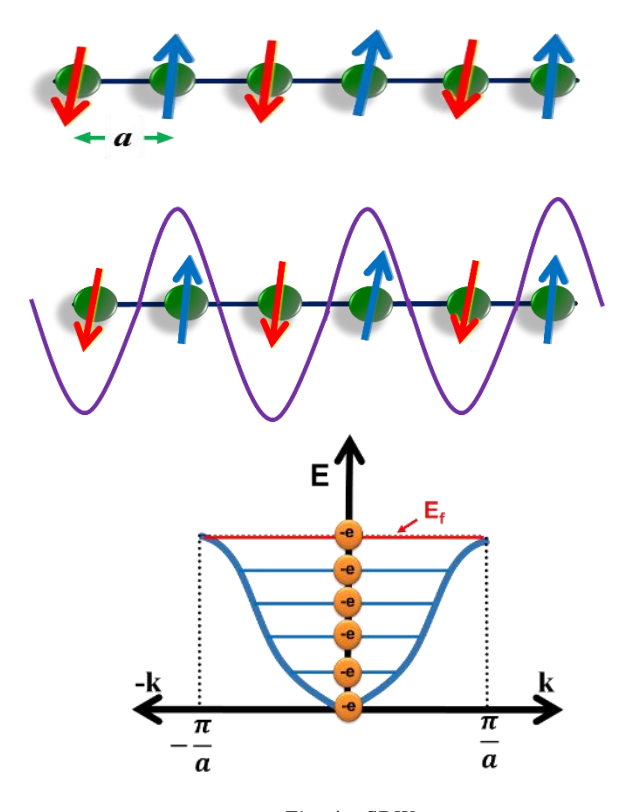


Fig. 4. SDW

the strong Coulomb interaction forbids the electrons from hopping from one site to another. Hence, this is an insulating state. This kind of insulator is called a Mott insulator. The Brillouin zone, in this case, is displayed in Fig. 4 (the bottom panel). Here the discontinuity (or the Fermi level) in the dispersion relation occurs at Brillouin zone boundaries, i.e., at $k = \pm \pi/a$.

(ii) Charge Density Wave (CDW)

the e-p interaction dominates over the e-e interaction (i.e., $g \gg U$), two electrons can form a bound state at a particular site. This is a bipolaronic state. At half-filling and in 1D systems, these bipolarons are formed at the alternate sites. In this case, the charge density varies periodically from site to site and therefore this state is called a Charge density wave state (middle panel of Fig. 5). Since bound pairs form at every other site, the unit cell becomes doubled and the phenomenon is referred to as dimerization. As a consequence of this dimerization, the Brillouin zone is reduced from $\left(-\frac{\pi}{a}, \frac{\pi}{a}\right)$ to $\left(-\frac{\pi}{2a}, \frac{\pi}{2a}\right)$ opening a gap at the Brillouin zone boundaries (bottom panel of Fig. 8). Due to this gap, the system again becomes insulating. This is known as the Peierls Instability and these kinds of insulators are referred to as the Peierls insulators [12].

Thus, it is clear from the above discussion that when the e-p coupling is small, GS of the HH system is an

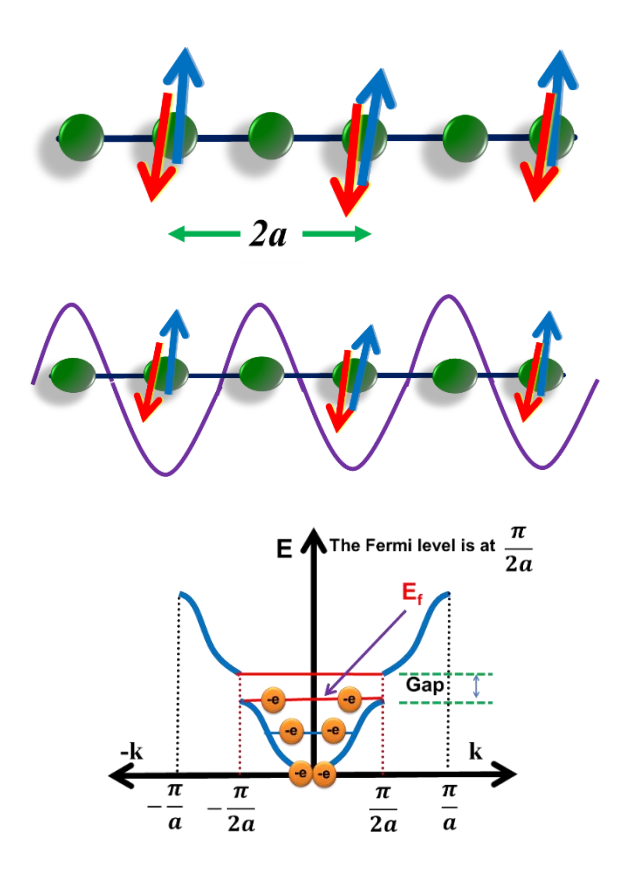


Fig. 5. CDW

SDW state and as the e-p coupling strength is sufficiently enhanced, the system goes into a CDW phase. This is not a good scenario superconductivity because to achieve high transition temperature one needs to have strong e-p interaction, while strong e-p interaction leads the system into a insulator. Thus, superconductivity CDW impossible in the HH model. Of course, one may be curious to study the transition region. Hirsch and Fradkin [13] performed a Monte-Carlo study of the HH model and showed that the transition from SDW phase to CDW phase is direct.

Later, Takada and Chatterjee (TC) [14] have taken up the 1D half-filled HH model for more critical investigation and studied the SDW-CDW transition in this system using a variational method coupled with the Bethe ansatz. Their analysis has revealed that there occurs a metallic phase at the crossover of the SDW-CDW transition. This result was obtained with the harmonic approximation for the lattice vibrations. The harmonic approximation means that the time period of the phonon oscillations is infinite which is the ideal condition and is not possible practically. So, to deal with the real materials we need to consider the finite lifetime effect for the phonons. This can be done by considering anharmonic phonons. In a later work [15], Chatterjee and Takada have performed their calculation including cubic and quartic anharmonicities in the lattice potential. Interestingly, their results show

that the width of the MP broadens in the presence of anharmonic phonons.

In the present thesis, we will present an improved variational calculation in order to obtain a more accurate nature of the phase transition in the HH model with a Gaussian phonon anharmonicity. Our results show that the thickness of the MP near the CDW-SDW crossover region is enhanced at the lower and moderate values of anharmonicity whereas as the anharmonicity is increased, the width of the MP eventually saturates.

1.8 Persistent currents

The persistent current is an interesting phenomenon that occurs at low temperature and in materials of mesoscopic dimensions. Persistent current is a current that flows continuously for an appreciable long period of time without any external source of power. The external power source works as a trigger for persistent current. Mesoscopic rings have grabbed much attention due to their interesting feature of carrying persistent currents. Büttiker et al. [16] have predicted that the persistent current can be observed experimentally in the microscopic rings. They also confirmed that the root cause for this kind of persistent current is the quantum phenomenon.

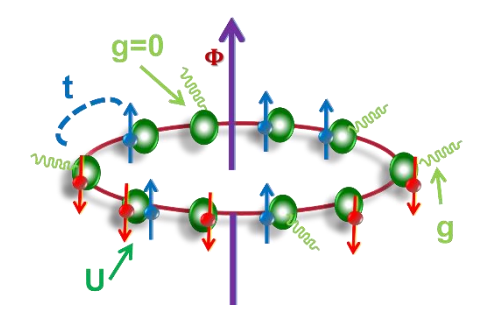


Fig. 6. A mesoscopic ring with the applied magnetic flux ϕ and with the terms, t, U and g.

Applying the magnetic field to the mesoscopic ring breaks the symmetry between the clockwise current and counter clockwise current. A ring with a diameter of 0.6 micrometres below 0.5 k temperature [17] can produce a current of 1 nano-ampere. Even the resistive materials can produce small persistent currents within them under the influence of an external magnetic field. Since, this current is of quantum origin, one needs to address the phase coherence effect of the electron's motion quantum mechanically. Aharonov-Bohm flux can be used to obtain persistent currents in a mesoscopic ring. The increase in the temperature is detrimental to the persistent current in the quantum rings.

There are two types of persistent currents. One is charge current and the other is the spin current. The charge current is due to the rate of change in charge whereas the spin current is due to the rate of change in the magnetization. The spin current is produced when the electrons with spin up and that with spin down are separated due to a potential. Usually, it occurs in a high spin-orbit coupling material.

1.9 Organization of Thesis

In Chapter 1, we introduce the basic concepts and the models that are necessary for the investigation of the problems presented in this thesis. To be more specific, we first presented a discussion on the Tightbinding model of energy bands and the Hubbard model. Then we introduced phonons, polarons and the Holstein model. Next we presented the Holstein-Hubbard model and discussed its spin-density and charge density wave phases. Finally we present a brief introduction to Persistent currents.

In Chapter 2, we present our work on the onedimensional Holstein-Hubbard model with Gaussian phonon anharmonicity at half filling. We use a variational technique based on a series of unitary transformations and employ a fairly accurate phonon state to average the transformed Holstein-Hubbard Hamiltonian to obtain an effective Hubbard model which is then solved using the exact Bethe – ansatz technique. Using the Mott-Hubbard criterion, local spin moment and the von Neumann entropy, we determine the ground state phase diagram and show the existence of an intermediate metallic phase flanked by the SDW and CDW phases.

Mesoscopic rings are interesting due to their property of exhibiting charge and spin persistent currents. Chapter 3 is dedicated to the calculation of persistent charge and spin currents in a finite mesoscopic ring with the magnetic flux threading into it. The system is modelled by the Holstein-Hubbard Hamiltonian so that the effect of interplay of *e-e* and *e-p* interactions on the persistent currents in mesoscopic rings can be studied. The model formulation, method and the results are discussed in the Chapter 3 elaborately.

In chapter 4, we summarize our results and present the concluding remarks.

References

- 1. J. C. Slater, G. F. Koster *Phys. Rev.* 94, no. 6, pp. 1498–1524, (1954).
- E.H. Lieb and F.Y. Wu, *Phys. Rev. Lett.* 20, no. 25, pp. 1445-1448, (1968); ibid. *physica A.* 321, pp. 1-27, (2003).
- 3. H. Shiba and P. A. Pincus, *Phys. Rev. B* **5**, 1966

- 4. N.F. Mott, *Proc. Phys. Soc. A.* **62**, pp. 416-422 (1949).
- J. Hubbard, Proc. Roy. Soc. Lon., Ser. A. Mat. Phys. Sci. 276, no. 1365, pp. 238-257, (1963); ibid. 277, no. 1369, pp. 237-259, (1964); ibid. 281, no. 1386, pp. 401-419, (1964).
- 6. T. Holstein, *Ann. Phys.* (*N.Y.*) **8**, pp. 325-342, (1959); ibid. **8**, pp. 343-389, (1959).
- 7. L. Landau, *Physik Zeitschrift Sowjetunion* **3**, pp. 664 (1933).
- 8. T.K. Mitra, A. Chatterjee and S. Mukhopadhyay, *Phys. Rep.* **153**, nos. 2 and 3, pp. 91-207, (1987). J. Devreese, arXiv:cond-mat/0004497v2 (2000); D. Emin, Polarons, Cambridge University Press.
- 9. L.D. Landau and S.I. Pekar, Translated and reprinted from Zh. Eksp. Teor. Fiz. **18**, No. 5, pp. 419–423 (1948)
- 10. H. Fröhlich, *Adv. Phys.* **3**, no. 11, pp. 325-361, (1954).
- 11. J. Bardeen, L. N. Cooper, and J. R. Schrieffer, *Phys. Rev.* **108**, no. 5, pp. 1175–1204, (1957).
- 12. R Peierls, More surprises in Theoretical Physics, Princeton University Press, (1991).

- 13. J. E. Hirsch and E. Fradkin *Phy. Rev. Let.* **49** 6 402-405 (1982).
- 14. Y. Takada and A. Chatterjee, *Phys. Rev. B.* **67**, pp. 081102 (1-4), (2003).
- 15. A. Chatterjee and Y. Takada, *J. Phys. Soc. Jap.* **73**, no. 4, pp. 964-969, (2004).
- 16. M. Büttiker, Y. Imry, R. Landauer, *Phys. Lett. A.* **96A**, no. 7, pp. 365-367, (1983).
- 17. A. C. Bleszynski-Jayich, et al., *Science.* **326**, pp. 272-275, (2009).

Phase transitions in one-Dimensional Hol	•

Chapter 2

Metallicity in a Holstein-Hubbard chain at half-filling with Gaussian anharmonicity

2.1. Introduction

The high-temperature superconductivity (HTS), after its discovery in the eighties, has continued to remain as one of the most interesting areas of research in the field of condensed matter physics. Several theories have been propounded to explain the origin of HTS in the cuprate superconductors. However no single theory has been able to explain all the properties of high-temperature superconductors satisfactorily. There have been quite a few theories which again advocated the *e-p* interaction as the mechanism for inducing pairing in high-temperature superconductors. The importance of *e-p* interaction in HTS has been reported

in several publications [1-11]. Plakida [5] has suggested that the high transition temperature T_c can be acquired even at the modest values e-p coupling strength. Alexandrov [6] has reported that a reasonable e-p coupling may lead to sufficient reduction in the polaron band, which may result in superconducting transition temperature. To examine superconductivity based on e-p coupling or the polaronic mechanism in the strongly correlated substances, the HH model appears to be the most preferred choice [8, 9, 12]. Later on, Sil et al. [9] and Sankar et al. [10] have studied the GS properties along with the phases of the extended HH model. However, the polaronic mechanism, though looks attractive at the first glance, runs into a problem if considered critically. It is plausible to assume that in order to have high T_c within the framework of the polaron mechanism, the material needs to have strong e-p coupling strength which however would push the system to the CDW state which is a non-metallic state. While in the case of sufficiently small *e-p* coupling, the onsite Coulomb correlation would be the dominant interaction and as a result the system then would be driven to the SDW phase which is again an insulating state. Thus, one expects that as the e-p interaction is raised, the system would go from a SDW state to a CDW state. Of course, one can still be curious to examine the nature of the crossover region. Hirsch and Fradkin [13] studied the nature of the transition region using the Monte-Carlo technique and reported that the SDW-CDW transition in the HH model is rather direct. Understandably, this result was a serious blow to the theories of HTS based on the polaronic mechanism.

In 2003, Takada and Chatterjee (TC) [14] have taken up the 1D half-filled HH model to give a critical relook at the transition region of this model. Their aim has been to examine analytically the nature of the transition region of the SDW and CDW phases. They have shown that, interestingly, the SDW-CDW transition in the 1D half-filled HH model is not direct. but goes through an intervening metallic phase. Krishna and Chatterjee (KC) [16] have examined the same problem with a better variational wave function [16,17] and have shown a modified variational analysis broadens the width of the intermediate conducting phase. Subsequently, a few other investigations have also corroborated the existence of this metallic phase [17-28]. Sankar and Chatterjee [10] have studied this problem by computing theoretically the von Neuman entropy that essentially measures the Quantum Entanglement (QE). Their calculation confirms the existence of the aforementioned intermediate metallic phase.

The works mentioned above considered the phonons to be harmonic which implies infinite lifetime for the phonons. However, the lattice potential is in general anharmonic and this anharmonicity introduces phonon-phonon interactions which bring in a finite life time effect for the phonons. So, to deal with the realistic cases, one needs to consider anharmonic phonons. Chatterjee and Takada (CT) [15] have examined the behaviour of the SDW-CDW crossover in the HH model incorporating the anharmonicity of phonons. Their investigation shows that anharmonicity broadens the width of intermediate metallic region.

The phonon state used by CT is however extremely simple. Also the phonon anharmonicity considered by them is only up to the fourth power in the lattice displacement. Konior [8] has contemplated a polaronic model with Gaussian anharmonicity and concluded that in this case the band reduction due to *e-p* coupling becomes much less. Furthermore, the results provided by Gaussian anharmonicity are convergent in all circumstances, a feature that is missing in the quartic and cubic anharmonicities [15].

In this chapter, we consider the 1D HH model with Gaussian anharmonic phonons and employ a more accurate phonon state (than that used by CT) to examine the effect of anharmonicity on the metallic phase at the SDW-CDW transition region employing the Mott criterion, local spin moment, double occupancy and the quantum entanglement.

2.2. The Model

The HH Hamiltonian is given by

$$H = H_{el} + H_{ph} + H_{el-ph}$$
 (2.1)

with

$$H_{el} = -t \sum_{\langle ij \rangle \sigma} c^{\dagger}_{i\sigma} c_{j\sigma} + U \sum_{i} n_{i\uparrow} n_{i\downarrow} , \qquad (2.1 a)$$

$$H_{ph} = \hbar\omega_0 \sum_{i} b_i^{\dagger} b_i + \lambda_{ap} \sum_{i} e^{-\gamma \left(b_i^{\dagger} + b_i\right)^2}, (2.1b)$$

$$H_{el-ph} = g \sum_{i\sigma} n_{i\sigma} (b_i^{\dagger} + b_i), \qquad (2.1c)$$

where $c_{i\sigma}^{\dagger}(c_{j\sigma})$ is the operator that creates (annihilates) an electron with spin σ at site i, t denotes the nearest-neighbour hopping parameter, $n_{i\sigma}$ (= $c_{i\sigma}^{\dagger}c_{i\sigma}$) refers to the number operator corresponding to the electron of spin σ at site i, U is the onsite Coulomb correlation energy, b_i^{\dagger} and b_i are the operators corresponding to creation and annihilation of phonons with dispersionless frequency ω_0 at site i,

 λ_{ap} and γ are respectively the strength and range of the lattice potential and g is the intra-site e-p interaction

2.3 Formulation

2.3.1 GS Energy

The above Hamiltonian contains the electronic and phononic terms which are coupled. One needs to change the basis to decouple the Hamiltonian. Canonical transformation is a way to transfer the Hamiltonian from one basis to another so that the Hamiltonian can be diagonalized. In the present case, however, the separation of electrons and phonons cannot be achieved exactly. We carry out a series of canonical transformation to approximately accomplish this purpose.

As a first step, we apply the variable-displacement Lang-Firsov (VDLF) transformation. The generator of this transformation can be written as

$$R_1 = \frac{g'}{\hbar\omega_0} \sum_i n_{i\sigma} (b_i^{\dagger} - b_i), \qquad (2.2)$$

where $g' = g \eta = \sqrt{\alpha} \eta$, α being the dimensionless e-p coupling constant and η a variational parameter. The

transformation (2.2) displaces the origin of the phonon oscillator. The conventional Lang-Firsov transformation is suitable in the anti-adiabatic regime. By considering the VDLF transformation, it is possible to treat the problem both in the adiabatic and anti-adiabatic regions. When η is close to 1, the VDLF transformation works well for the anti-adiabatic case, while for $\eta \to 0$, it is good for the adiabatic regime. Thus, by considering the VDLF transformation, we can cover the entire range of adiabaticity i.e., both adiabatic and anti-adiabatic regions.

As a result of the VDLF transformation, H reduces to

$$H_1 = e^{R_1} H e^{-R_1} \,. {(2.3)}$$

The above transformed Hamiltonian can be calculated using the Baker-Campbell-Hausdorff (BCH) formula:

$$e^{R}Ae^{-R} = A + [R,A] + \frac{1}{2}[R,[R,A]] + \frac{1}{3!}[R,[R,R,A]] + \cdots$$
 (2.4)

Using the BCH formula, we obtain

$$\begin{split} H_1 &= -t \sum_{i,i+\delta,\sigma} e^{\left(x_{i\sigma} - x_{i+\delta,\sigma}\right)} C_{i\sigma}^{\dagger} C_{i+\delta,\sigma} + U \sum_i n_{i\uparrow} n_{i\downarrow} \\ &+ \hbar \omega_0 \sum_i b_i^{\dagger} b_i - g' \sum_{i\sigma} \left(b_i^{\dagger} + b_i\right) n_{i\sigma} \end{split}$$

$$+\frac{(g')^{2}}{\hbar\omega_{0}}\left(\sum_{i\sigma}n_{i\sigma}^{2}+2\sum_{i}n_{i\uparrow}n_{i\downarrow}\right)+g\sum_{i\sigma}n_{i\sigma}\left(b_{i}^{\dagger}+b\right)$$
$$-\frac{2gg'}{\hbar\omega_{0}}\sum_{i\sigma}n_{i\sigma}^{2}-\frac{4gg'}{\hbar\omega_{0}}\sum_{i}n_{i\uparrow}n_{i\downarrow}$$
$$+\lambda_{ap}\sum_{i\sigma}e^{-\gamma\left(b_{i}^{\dagger}+b_{i}-\frac{2g'}{\hbar\omega}\sum_{\sigma}n_{i\sigma}\right)^{2}}\left(2.5\right)$$

The transformation (2.2) deals with the displacements of the phonon coordinates that depend on the electron concentrations at particular sites. One can also have phonon displacements that are independent of electron concentration. This feature was captured by the Takada-Chatterjee transformation [14]. The generator of this transformation is given by:

$$R_2 = \sum_{k} [h(b_k^{\dagger} - b_k)]$$
 (2.6)

where h has to be obtained variationally. After applying this transformation, the Hamiltonian becomes

$$H_2 = e^{R_2} H_1 e^{-R_2} (2.7)$$

$$H_{2} = \sum_{i\sigma} \left(2g'h + \frac{(g')^{2}}{\hbar\omega_{0}} - 2gh - \frac{2gg'}{\hbar\omega_{0}} \right) n_{i\sigma}$$

$$-t \sum_{ij\sigma} e^{\frac{g'}{\hbar\omega_{0}} \left(\left(b_{i}^{\dagger} - b_{i} \right) - \left(b_{j}^{\dagger} - b_{j} \right) \right)} C_{i\sigma}^{\dagger} C_{j\sigma}$$

$$+ \sum_{i} \left(U + \frac{2(g')^{2}}{\hbar\omega_{0}} - \frac{4gg'}{\hbar\omega_{0}} \right) n_{i\uparrow} n_{i\downarrow}$$

$$+ \sum_{i\sigma} (g - g') (b_{i}^{\dagger} + b_{i}) n_{i\sigma}$$

$$+ \hbar\omega_{0} \sum_{i} \left(b_{i}^{\dagger} b_{i} - h(b_{i}^{\dagger} + b_{i}) + h^{2} \right)$$

$$+ \lambda_{ap} \sum_{i\sigma} e^{-\gamma \left(b_{i}^{\dagger} + b_{i} - 2h - \frac{2g'}{\hbar\omega_{0}} \sum_{\sigma} n_{i\sigma} \right)^{2}} (2.8)$$

Next we apply the Squeezing transformation [14,15] given by

$$R_3 = \alpha' \sum_{k} \left(b_k b_k - b_k^{\dagger} b_k^{\dagger} \right) \qquad (2.9)$$

When a phonon is emitted by an electron, the electron recoils according to the law of conservation of linear momentum. If another phonon is emitted by the recoiling electron, then

there will be a correlation between these two successively emitted phonons. The squeezing transformation (2.9) is known to capture the effect of these phonon correlations. The squeezing transformation also incorporates some effect of phonon anharmonicity. Here, α' is the variational parameter.

After applying the squeezing transformation, the transformed Hamiltonian can be written as:

$$H_3 = e^{R_3} H_2 e^{-R_3} (2.10)$$

$$\begin{split} H_{3} &= \sum_{i\sigma} \left(-2h(g-g') - \frac{g'}{\hbar\omega_{0}} (2g-g') \right. \\ &+ (g-g')e^{2\alpha'} \left(b_{i}^{\dagger} + b_{i} \right) \\ &+ \lambda_{ap} e^{-\gamma \left\{ \left(b_{i}^{\dagger} + b_{i} \right)e^{2\alpha'} - 2h - \frac{2g'}{\hbar\omega_{0}} \right\}^{2} \right. \\ &- \lambda_{ap} e^{-\gamma \left\{ \left(b_{i}^{\dagger} + b_{i} \right)e^{2\alpha'} - 2h \right\}^{2} \right)} n_{i\sigma} \end{split}$$

$$+ \sum_{i} \left(\cup -\frac{2g'}{\hbar \omega_{0}} (2g - g') + \lambda_{ap} e^{-\gamma \left\{ \left(b_{i}^{\dagger} + b_{i} \right) e^{2\alpha'} - 2h - \frac{4g'}{\hbar \omega_{0}} \right\}^{2}} - 2\lambda_{ap} e^{-\gamma \left\{ \left(b_{i}^{\dagger} + b_{i} \right) e^{2\alpha'} - 2h - \frac{2g'}{\hbar \omega_{0}} \right\}^{2}} + \lambda_{ap} e^{-\gamma \left\{ \left(b_{i}^{\dagger} + b_{i} \right) e^{2\alpha'} - 2h \right\}^{2}} \right) n_{i} n_{i}$$

$$- t \sum_{\langle i,j \rangle \sigma} e^{\frac{g'}{\hbar \omega_{0}} \left\{ \left(b_{i}^{\dagger} - b_{i} \right) - \left(2b_{j}^{\dagger} - b_{j} \right) \right\} e^{2\alpha'}} c_{i\sigma}^{\dagger} c_{j\sigma}$$

$$+ \hbar \omega_{0} \sum_{i} \left(\frac{1}{4} e^{4\alpha'} (b_{i}^{\dagger} + b_{i})^{2} - \frac{1}{4} e^{-4\alpha'} (b_{i}^{\dagger} - b_{i})^{2} - \frac{1}{2} - h (b_{i}^{\dagger} + b_{i}) e^{2\alpha'} + h^{2} \right)$$

$$+ \lambda_{ap} \sum_{i} e^{-\gamma \left\{ \left(b_{i}^{\dagger} + b_{i} \right) e^{2\alpha'} - 2h \right\}^{2}} (2.11)$$

We assume that after the above three unitary transformation, the residual electron-phonon interactions have become sufficiently weak so that the total wave function of H_3 may be given by the simple product of the electronic and phonon functions. Thus we write the total wave function of H_3 as:

$$|\psi\rangle = |\psi_p\rangle|\psi_e\rangle \tag{2.12}$$

Then the energy of the system is given by:

$$E = \langle \psi | H_3 | \psi \rangle = \langle \psi_e | \langle \psi_p | H_3 | \psi_p \rangle | \psi_e \rangle$$
$$= \langle \psi_e | H_{eff} | \psi_e \rangle, \tag{2.13}$$

where

$$H_{eff} = \langle \psi_p | H_3 | \psi_p \rangle \tag{2.14}$$

To calculate H_{eff} , we choose $|\psi_p\rangle$ as:

$$|\psi_p\rangle = \sum_{n=0}^{M} c_n |\varphi_n(x)\rangle,$$
 (2.15)

where $|\varphi_n(x)\rangle$ is the nth excited state eigenfunction of a simple harmonic oscillator with the frequency ω_0 .

$$\varphi_n(x) = \left(\frac{\sqrt{\omega_0}}{\sqrt{\pi\hbar} \ 2^n \ n!}\right)^{1/2} H_n\left(\sqrt{\frac{\omega_0}{\hbar}} \ x\right) e^{-\frac{\omega_0}{2\hbar} x^2}, \quad (2.16)$$

where H_n is the Hermite polynomial of order n. The effective electronic Hamiltonian is finally obtained as

$$\begin{split} H_{eff} &= -t_{eff} \sum_{\langle ij \rangle \sigma} c_{i\sigma}^{\dagger} c_{j\sigma} + U_{eff} \sum_{i} n_{i\uparrow} n_{i\downarrow} \\ &+ \varepsilon_{eff} \sum_{i\sigma} n_{i\sigma} + N \lambda_{ap} E_{1} \\ &+ N \hbar \omega_{0} \left(\frac{1}{4} e^{4\alpha'} S_{2} - \frac{1}{4} e^{-4\alpha'} S_{3} - \frac{1}{2} + h^{2} \right. \\ &- h e^{2\alpha'} S_{1} \right), \end{split} \tag{2.17}$$

with

$$\varepsilon_{eff} = -\frac{(2g - g')}{\hbar \,\omega_0} + (g - g') (e^{2\alpha'} S_1 - 2h) + \lambda_{ap} (E_2 - E_1), \qquad (2.17 \text{ a})$$

where
$$g'=g\,\eta=\sqrt{\alpha}\,\eta,$$

$$t_{eff}=t\,F^2, \qquad (2.17~{\rm b})$$

$$U_{eff}=U-\frac{2g'}{\hbar\,\omega_0}(2g-g')$$

$$+\lambda_{ap}(E_3 - 2E_2 + E_1),$$
 (2.17 c)

$$S_{i} = \sum_{k,l=0}^{M} c_{kl} \int_{-\infty}^{\infty} e^{-y^{2}} \xi_{i}(y) H_{k}(y) H_{l}(y) dy, (2.17d)$$

$$F = \sum_{k,l=0}^{M} c_{kl} e^{-a^2/4} \int_{-\infty}^{\infty} e^{-y^2} H_k \left(y + \frac{a}{2} \right) \left(y - \frac{a}{2} \right) dy,$$
(2.17 e)

$$E_{i} = \sum_{k,l=0}^{M} c_{kl} \int_{-\infty}^{\infty} e^{-y^{2} - \gamma \left(\sqrt{2} y e^{2\alpha'} - 2h - \zeta_{i}\right)^{2}}$$

$$\times H_k(y)H_l(y)dy$$
, (2.17f)

where

$$c_{kl} = c_k c_l \sqrt{1/2^{k+l} k! \ l! \ \pi} ,$$
 (2.17g)

$$\xi_1 = \sqrt{2} y$$
, (2.17h)

$$\xi_2 = 2y^2,$$
 (2.17i)

$$\xi_3 = 2(y^2 - 2l - 1),$$
 (2.17j)

$$\zeta_1 = 0, \tag{2.17k}$$

$$\zeta_2 = \frac{2g'}{\hbar\omega_0},\tag{2.17l}$$

$$\zeta_3 = \frac{4g'}{\hbar\omega_0} \quad , \tag{2.17m}$$

for i = 1, 2 and 3.

In general, the onsite GS energy, the hopping parameter and the onsite Coulomb interaction are modified due to the polaronic effect. Because of polaron formation, the hopping parameter t is scaled down by a factor which is called the Holstein reduction factor. The polaron formation thus reduces the width of the energy band. Besides t, U and g, several other parameters such as filling factor, size and the dimensionality of the system also tend to play a vital part in dictating the phases of the HH model. In this thesis, we consider only a 1D system.

As we can see, the parameters ε , U and t are renormalized as ε_{eff} , U_{eff} and t_{eff} respectively. The Hamiltonian H_{eff} (Eq. (2.17)) represents an effective Hubbard Model (with a few constant terms) which can be solved by following Lieb and Wu [30] who applied the nested Bethe-Ansatz (BA) technique to solve exactly the 1D half-filled Hubbard Model. Using the BA technique, the exact GS energy per electron (ε) corresponding to H_{eff} at half filling is obtained as:

$$\varepsilon = \frac{1}{4} e^{4\alpha'} S_2 - \frac{1}{4} e^{-4\alpha'} S_3 - \frac{1}{2} - h e^{2\alpha'} S_1$$

$$+ h^2 + \lambda_{ap} E_1 - J + \frac{U_{eff} - |U_{eff}|}{4}$$

$$- \int_0^\infty \frac{4 t_{eff} J_0(\xi) J_1(\xi) d\xi}{\xi \left[1 + exp \left(\xi \frac{|U_{eff}|}{2 t_{eff}} \right) \right]}, \quad (2.18)$$

where

$$J = (2g - g')g' - (g - g')[e^{2\alpha'}S_1 - 2h] + \lambda_{an}E_1 - \lambda_{an}E_2. \quad (2.18a)$$

We have modified Bethe ansatz by adding a new term $(U_{eff} - |U_{eff}|)/4$ so that the solution is applicable even for negative U_{eff} .

To determine the GS energy, we perform numerical minimization of Eq. (2.18) with respect to η , h and α' . The average lattice displacement (ALD) is given by

$$\langle x_i \rangle = e^{2\alpha'} \left(S_1 / \sqrt{2} - \sqrt{2} g' - \sqrt{2} h \right).$$
 (2.19)

2.3.2. Local spin moment (LSP)

Calculating the local spin moment (LSP) will help us in determining the quantum phases of the system. If the system is in the SDW state, an electron occupying a particular site will be unpaired and the local spin moment per site will be high. On the other hand, if the local spin moment is zero, the sites are either empty or doubly occupied. This will correspond to the CDW state. The average electron spin moment per site can be measured by:

$$L_0 = \frac{1}{N} \sum_{i} \langle S_i^2 \rangle$$

$$= \frac{3}{4} - \frac{3}{2N} \sum_{i} \langle n_{i\uparrow} n_{i\downarrow} \rangle , \qquad (2.20)$$

which on using the expression for variational GS energy yields

$$L_0 = \frac{3}{4} - \frac{3}{2} \frac{d\varepsilon}{dU}$$
 (2.21)

It can be shown [14-17] that for completely uncorrelated electrons, L_0 is equal to 3/8 (= 0.375). Furthermore, it is also known that for the Hubbard model, L_0 can vary between 3/8 (which is the band limit) and 3/4 (which is the atomic limit).

2.3.3. Entanglement Entropy (EE)

Quantum Entanglement (QE) is one of the most striking phenomena in Quantum Mechanics and is also known to be related to Quantum Phase Transition (QPT) [31-36] which happens due mainly to quantum fluctuations. In this section, we wish to study the QPTs that are associated with the HH model using the idea of QE which can be measured by calculating the Entanglement Entropy (EE) such as the von Neumann entropy. It has been found that the higher is the entanglement, the higher is the conduction. Hence, one can conclude the existence of a metallic state from the calculation of the entanglement entropy.

In the 1D HH model, one can conceive of four states namely, $|0\rangle$, $|\uparrow\rangle$, $|\downarrow\rangle$ and $|\uparrow\downarrow\rangle$. The von Newmann entropy is then given by:

$$E_{\vartheta} = -Tr(\rho_r \log_2 \rho_r), \qquad (2.22)$$

where ρ_r represents the reduced density matrix which for the present case can be written as:

$$\rho_r = \omega_e | 0 \rangle \langle 0 | + \omega_\uparrow | \uparrow \rangle \langle \downarrow | + \omega_\downarrow | \downarrow \rangle \langle \uparrow | + \omega_{\uparrow\downarrow} | \uparrow \downarrow \rangle \langle \uparrow \downarrow |, \qquad (2.22a)$$

where $\omega_{\uparrow\downarrow}$ denotes the double occupancy and is given by

$$\omega_{\uparrow\downarrow} = \langle n_{i\uparrow} n_{i\downarrow} \rangle \equiv \omega$$
 (2.22b)

and ω_{\uparrow} , ω_{\downarrow} and ω_{e} are given by

$$\omega_{\uparrow} = \omega_{\downarrow} = (n/2) - \omega_{\uparrow\downarrow}$$
 (2.22c)

$$\omega_e = 1 - \omega_{\uparrow} - \omega_{\downarrow} - \omega_{\uparrow\downarrow}.$$
 (2.22d)

The entanglement entropy E_{ϑ} can be finally determined by exploiting the Hellmann-Feynman theorem

$$\frac{\partial \varepsilon}{\partial U} = \langle n_{i\uparrow} n_{i\downarrow} \rangle. \tag{2.23}$$

2.4 Numerical Results and Discussion

For the numerical analysis, we study three cases of anharmonicity: Case (i) λ_{ap} = 0.05, γ = 0.05; Case (ii) λ_{ap} = 0.2, γ = 0.05 and Case (iii) λ_{ap} = 0.75, γ = 0.5 and set the value of $\hbar\omega_0$ equal to 1. (i) refers to a small anharmonic case, (ii) refers to a moderate anharmonic case and (iii) refers to a high anharmonic case. We shall work in the anti-adiabatic region and consider t =

 $0.2 \omega_0$ in this chapter. We have found that M = 3 gives the convergent result for the GS energy.

Fig. 1 displays the behaviour of the GS energy per site with respect to the on-site e-e strength (U) for both harmonic and anharmonic lattices. At large U, the anharmonicity increases the energy while for $U \le 1$, it appears to have much less influence. The TC results [13] are exactly reproduced in the harmonic case $(\lambda_{ap} = \gamma = 0)$.

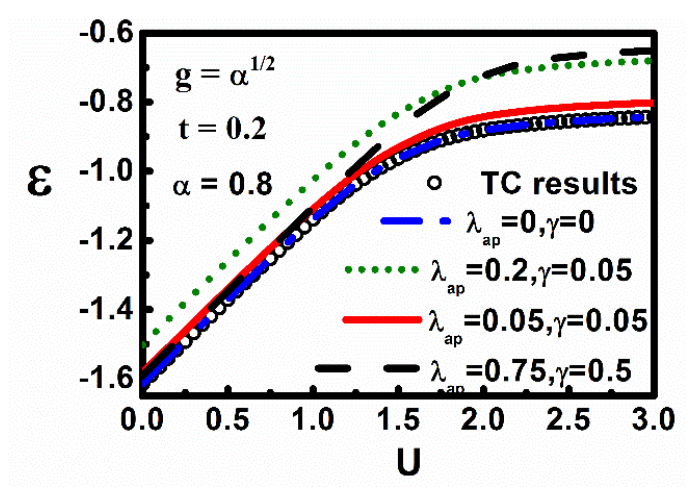
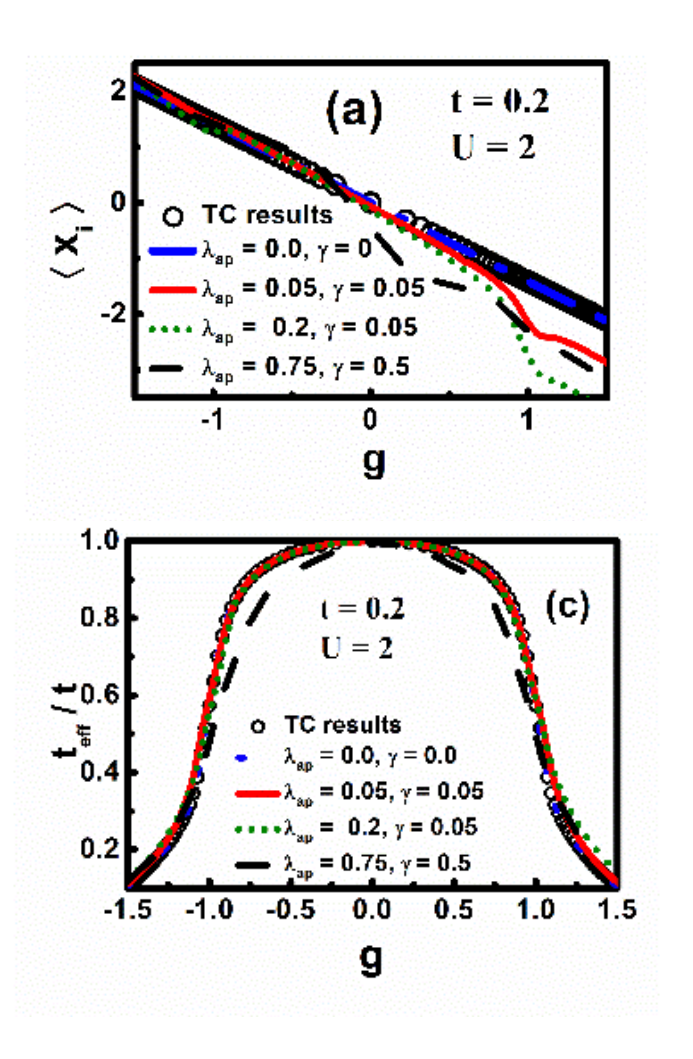


Fig. 1. GS energy (ε) vs. onsite Coulomb correlation strength U.

Fig. 2(a) shows how $\langle x_i \rangle$ behaves with the variation in the *e-p* coupling strength g. The value of $\langle x_i \rangle$

diminishes with rising g. For the case: $\lambda_{ap} = 0 = \gamma$, the present results agree well with the TC results [14] lending credence to the TC results. However, for a substantially large anharmonicity, the behaviour of $\langle x_i \rangle$ is rather complex and appears to be asymmetric in g. Fig. 2(b) describes the behaviour of the optimized η versus g. We notice that there is an essential qualitative difference in the way η behaves with respect to g for a sufficiently high anharmonicity. To be more specific, η first decreases with increasing g, develops a minimum at some critical g and then increases with further increase in g and reaches a saturation value which is the strong-coupling limit. Fig. 2(c) reveals that with the increase in g, the band becomes rapidly and continuously narrower. For strong anharmonicity, the band reduction is even more rapid. Fig. 2(d) displays the decrease in the effective on-site e-e interaction as gincreases. The presence of anharmonicity reduces U_{eff} much further. One may note that for the harmonic case, $\langle x_i \rangle = -\sqrt{2}g$, with $g = \sqrt{\alpha}$, α being the dimensionless e-p coupling constant.

The increase in the anharmonicity causes a deviation in the harmonic value of $\langle x_i \rangle$ for positive g. Though the deviation is not very systematic, it looks more pronounced at higher g values. The shift in $\langle x_i \rangle$ is accompanied with the reduction in U_{eff} , t_{eff}/t and L_0 which is a consequence of the increase in the



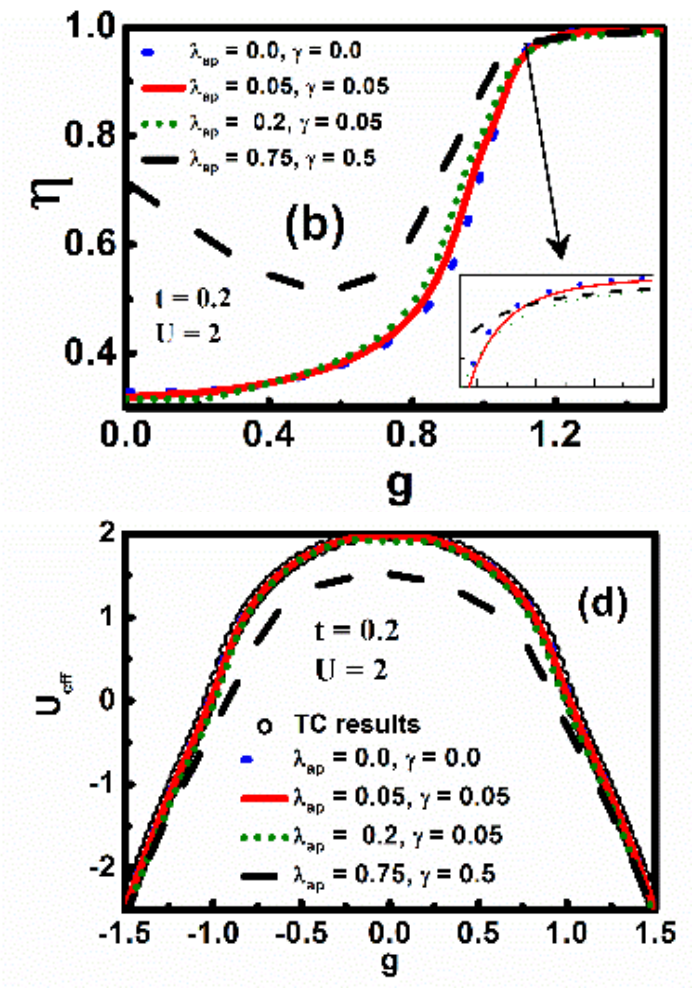


Fig. 2. (a) $\langle x_i \rangle$ as a variation of g for different λ_{ap} and γ values. (b) η versus g. (c) t_{eff}/t versus g. (d) U_{eff} variation with g.

optimized η from its value in the harmonic case. As g is increased beyond 1.1, the anharmonicity brings down η which consequently enhances t_{eff}/t giving rise to the creation of polarons that are mobile. The decrease in η also happens because of the competition between the e-e and e-p couplings. For a considerably large anharmonicity, the onsite e-p coupling becomes strong enough to dominate over the onsite e-e Coulomb repulsion.

In Fig. 3(a), t_{eff}/t is plotted against U for three different anharmonic cases. The harmonic case, as expected, compares well with the TC results. As U is made considerably large, t_{eff}/t approaches 1. The graph for the variation of dt_{eff}/dU with U in Fig. 3(b) displays a double-peak structure as observed in the case of harmonic lattice, though the peaks are higher in the case of larger anharmonicity. Furthermore, as the anharmonicity is increased, the peaks move to the right. This happens because the phonon anharmonicity enhances the e-p interaction strength and consequently, a stronger Coulomb correlation is needed to bring about the transition exhibited by the double-peak structure.

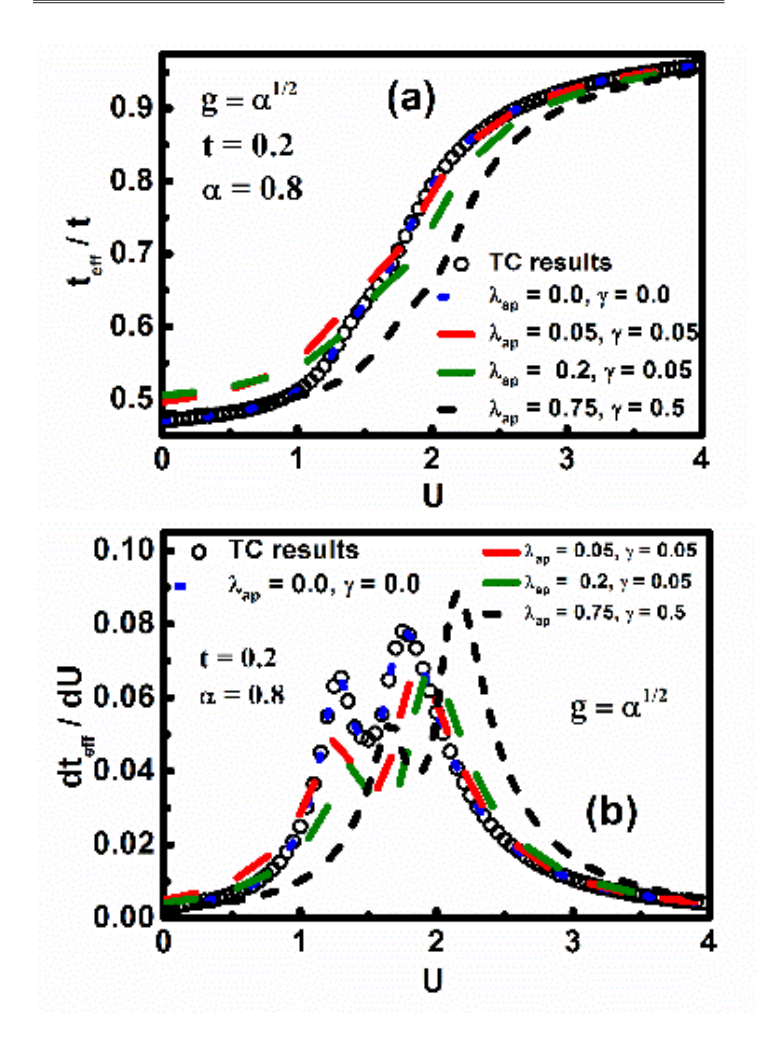


Fig. 3 (a) t_{eff}/t vs. U. (b) dt_{eff}/dU vs. U.

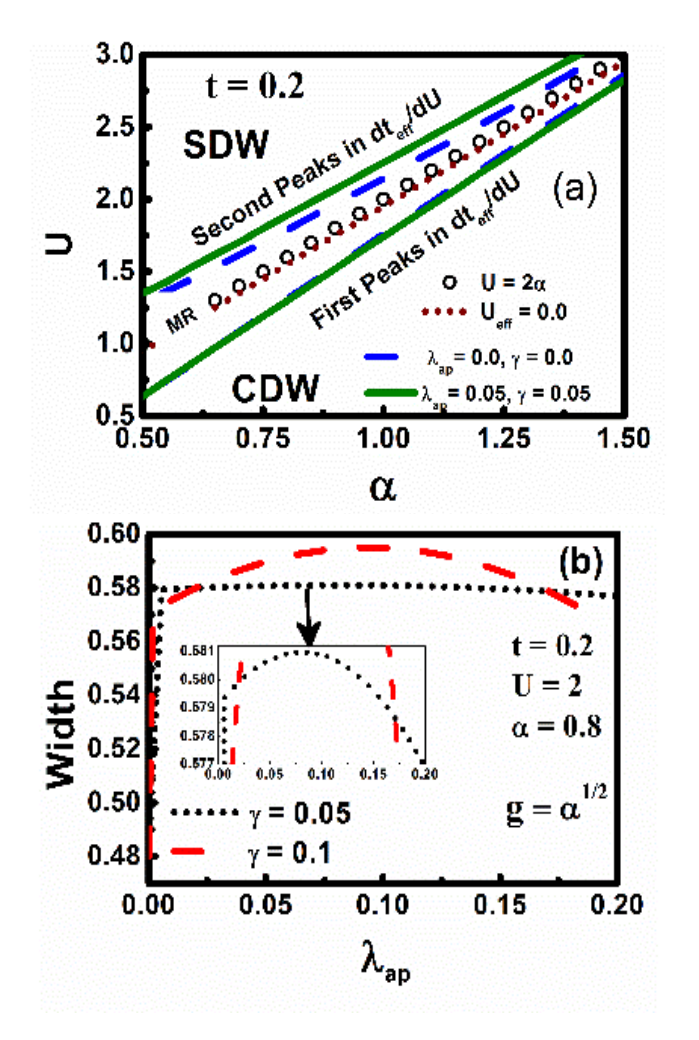


Fig. 4(a) Phase diagram in $\alpha - U$ plane ascertained from the peaks in dt_{eff}/dU . MR: metallic region (b) Peak-to-peak width(from dt_{eff}/dU -U-graph) vs λ_{ap} for two different values of γ .

Fig. 4(a) provides the phase diagram in the $\alpha - U$ plane as obtained from the peaks of the dt_{eff}/dU versus U —graph. The role of anharmonicity on MP is displayed in Fig. 4(b) for two different cases. For the harmonic system, the width of MP is 0.48 (in units of ω_0). As the Gaussian anharmonicity is switched on, the width of MP broadens rapidly to the value 0.58 (in units of ω_0). As the strength of anharmonicity is raised further, the width keeps on increasing, reaches a maximum value and then becomes thinner as the anharmonicity is further increased.

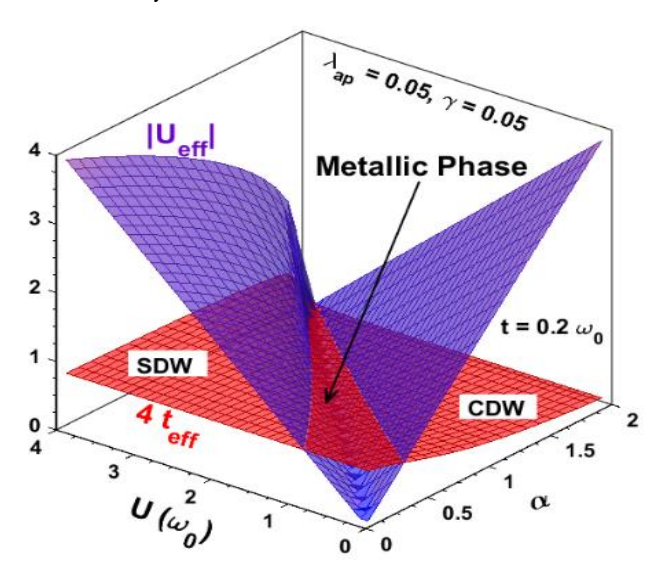


Fig. 5. A 3-dimensional picture depicting the behavior of $|U_{eff}|$ (blue) and $4t_{eff}$ (red) with U and a.

Fig. 5 provides a 3D illustration of MP that occurs at the SDW-CDW transition area for a given λ and γ . The red surface flanked by the two surfaces in blue satisfies the MP condition: $4t_{eff} \gtrsim |U_{eff}|$ accordingly represents the metallic phase. We observe that the value of U_{eff} is positive on the left side of MR and so this region would be in the SDW phase. On the right side of MR, however, U_{eff} turns out to be negative which implies that the region on the right side of MP would be in the CDW phase. We therefore infer that an increase in α leads the system to undergo a transition from an insulating antiferromagnetic SDW phase to the insulating CDW phase through a conducting region. This is indeed an important observation because it implies that even when the e-p coupling is strong, the system parameters can be manipulated to obtain a metallic GS which can go to a superconducting phase if temperature is lowered. Fig. 4(b) suggests that moderate Gaussian anharmonicity is most conducive for superconductivity.

Fig. 6(a) displays the dependence of LSP (L_0) on g for with different sets of λ_{ap} and γ . L_0 has a finite value at g=0 and remains almost independent of g up to a certain value of g, after which L_0 drops off rather sharply to zero. The reason is easy to understand. At small g, as

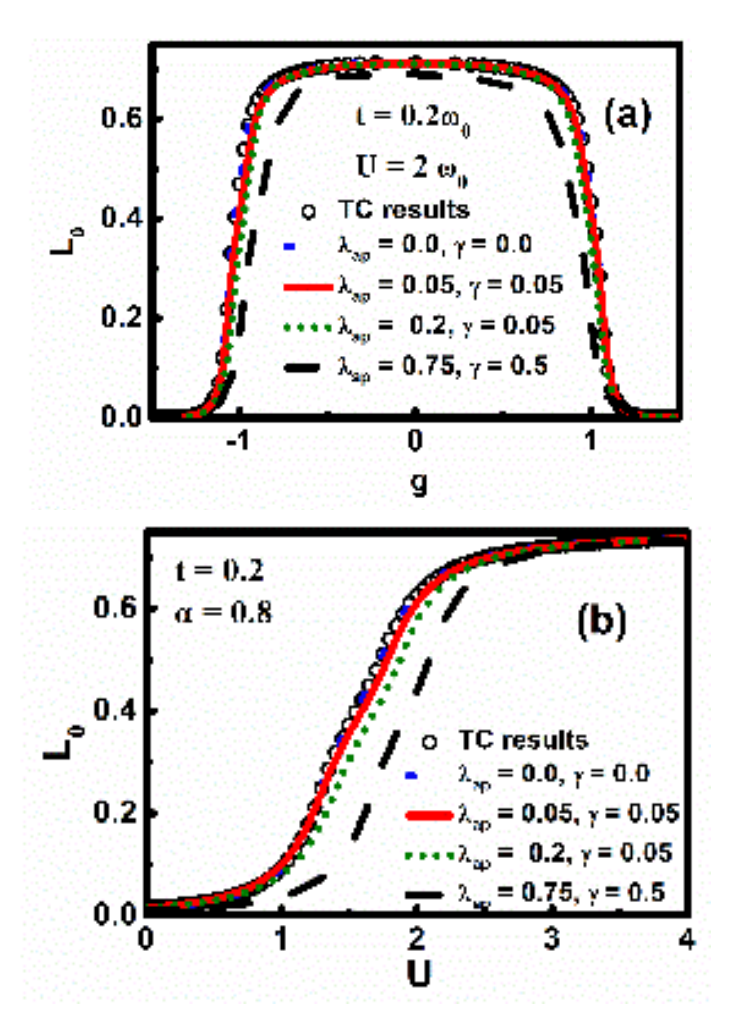


Fig. 6(a) L_0 versus g (b) L_0 versus U for different values of λ_{ap} and γ .

increases, the effective hopping parameter changes very slightly and as a result, L_0 shows no perceptible change in its value. However, as g is increased beyond a particular value, L_0 falls off sharply to zero. The reason is again not difficult to understand. For a substantially high value of g, U_{eff} can become negative and consequently a pair of electrons can inhabit a single site. This makes L_0 equal to zero. L_0 is suppressed considerably in the case of higher anharmonicity. On the other hand, in the cases of low and moderate anharmonicities, the suppression of L_0 is only marginal. Fig. 6(b) displays the behaviour of L_0 with respect to U. As U increases, the electronelectron repulsion becomes stronger and as a result it becomes difficult for two electrons to occupy a particular site. This leads to a larger value of L_0 for any atomic site. Up to $U \approx 1$, no perceptible change is observed in L_0 while on the contrary, for $1 \lesssim U \lesssim$ 2.2, it goes through a monotonic increase. As U is further increased, L_0 approaches essentially a finite saturation value.

Fig. 7. displays the 3D surface graph of L_0 with respect to U and α , while Fig. 8. shows the contour graphs of L_0 in the U- α plane. For an absolutely free electron gas which is uncorrelated, L_0 = 0.375. It is observed that each point in the intermediate phase of Fig. 8. corresponds to the value, L_0 = 0.375. Thus, this

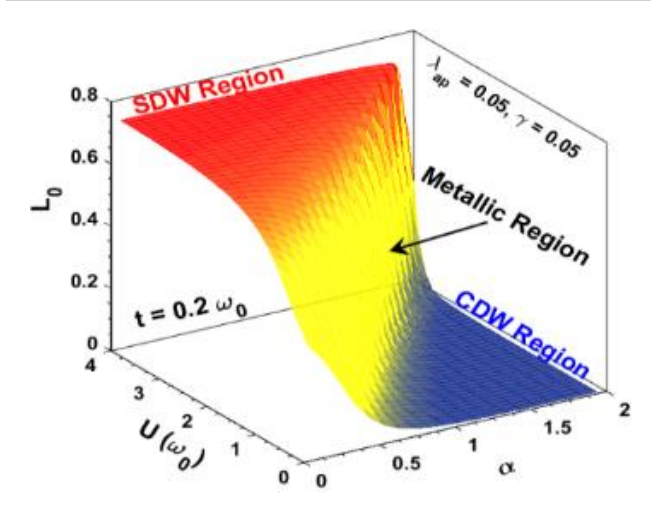


Fig. 7. L_0 versus U for $\lambda_{ap}=0.05$, $\gamma=0.05$ and t=0.2 ω_0 .

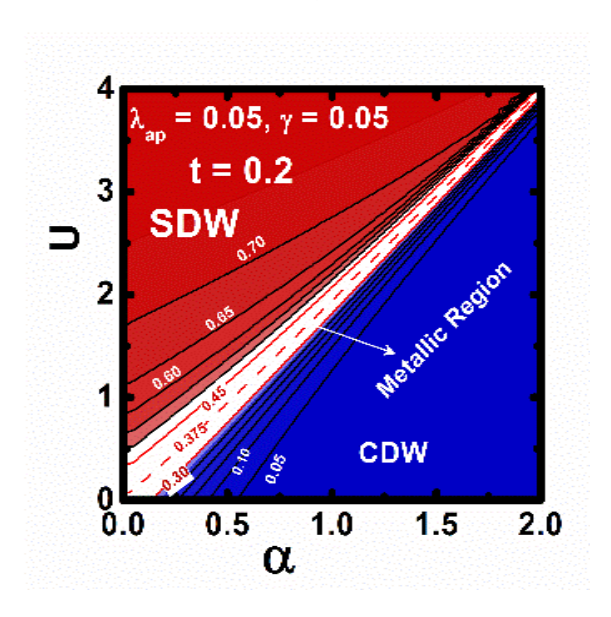
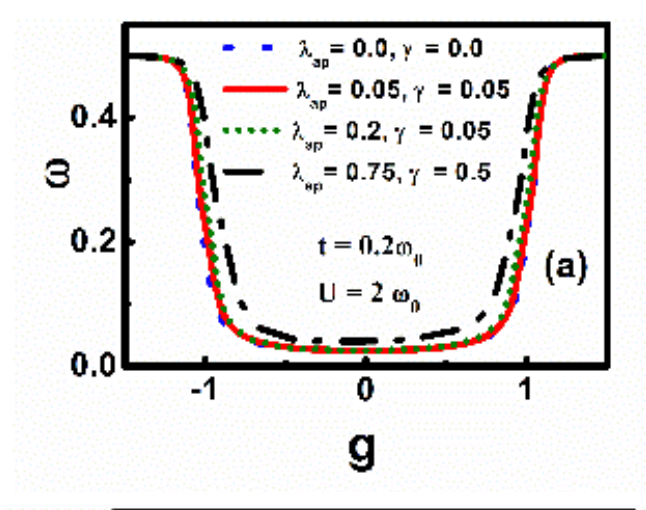
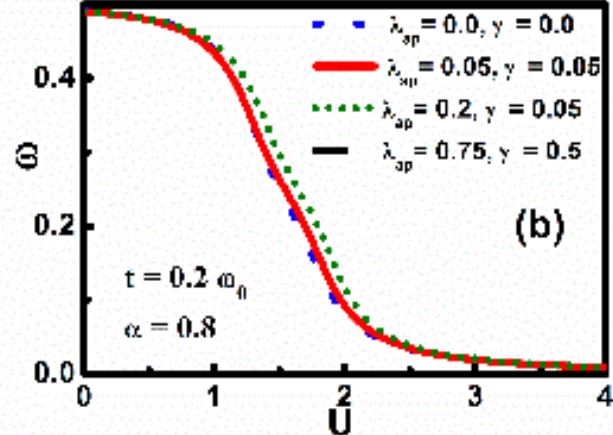


Fig. 8. Contour plots of L_0 in a - U plane.





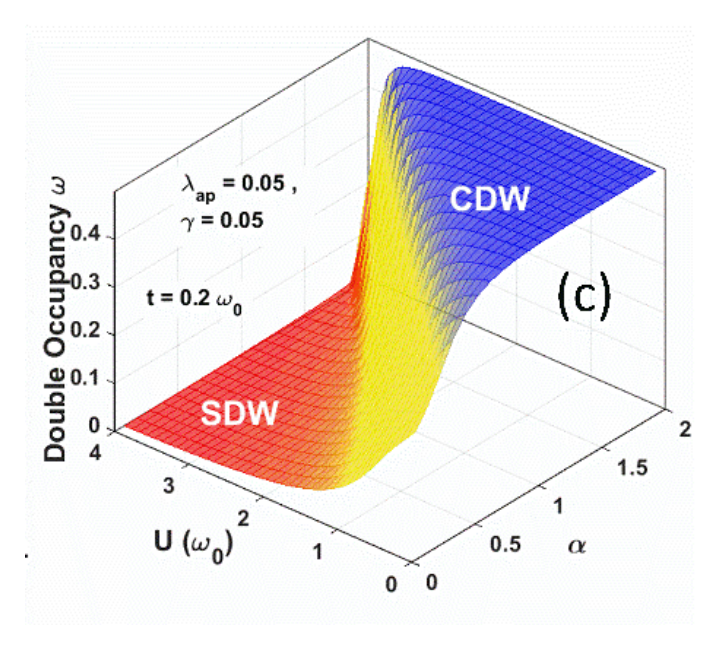
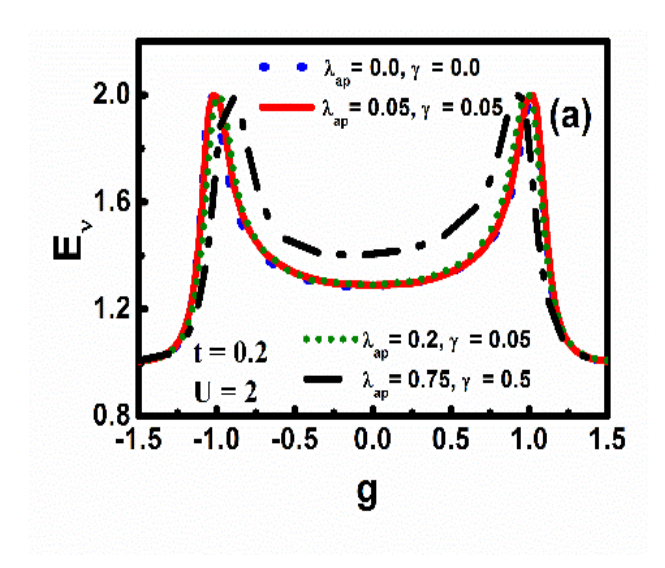


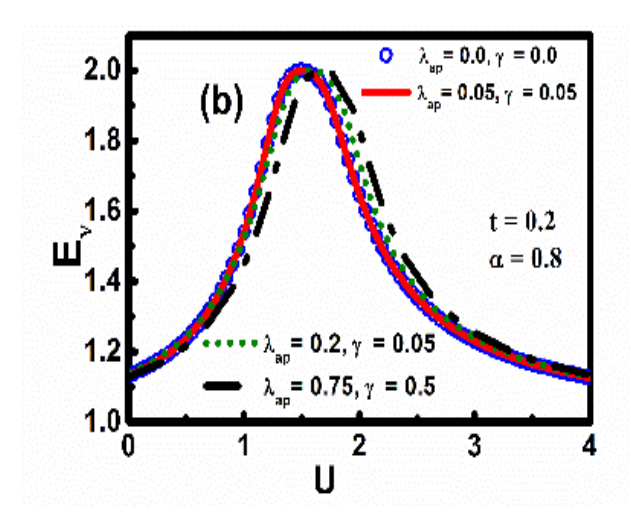
Fig. 9. (a) ω versus g. (b) ω versus U. (c) 3D plot of ω in the (U, a) plane.

observation gives another evidence which corroborates the result that there may exist a metallic state in between the SDW and CDW phases.

Fig. 9(a). describes the behaviour of the double occupancy ω , versus g for several values of λ_{ap} . When g has is small but a positive value, the double occupancy ω turns out to be small. This corresponds to an SDW state. A rise in g causes a rapid rise in ω and above a critical value of λ_{ap} , ω reaches a constant saturation value implying the formation of bipolarons. This corresponds to the CDW state. With increasing

anharmonicity, the rise in ω is rather marginal and that too happens at lower values of g. Fig. 9(b) displays the behaviour of ω versus U. At a sufficiently low value of U, U_{eff} has a negative value. This gives rise to a higher value of ω , which consequently implies the formation of a bipolaron or a CDW state. On the contrary, with increase in U, U_{eff} acquires a positive value. This reduces ω and with sufficient increase in U, ω approaches zero which represents the SDW state. Fig. 9(c) displays the 3-dimensional variation of ω with respect to U and α .





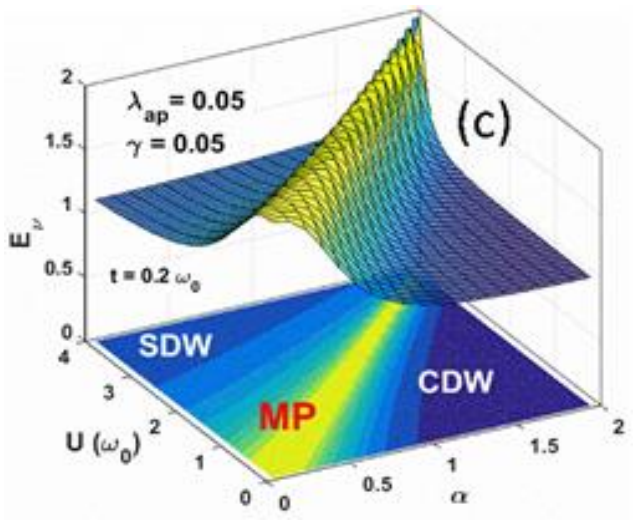


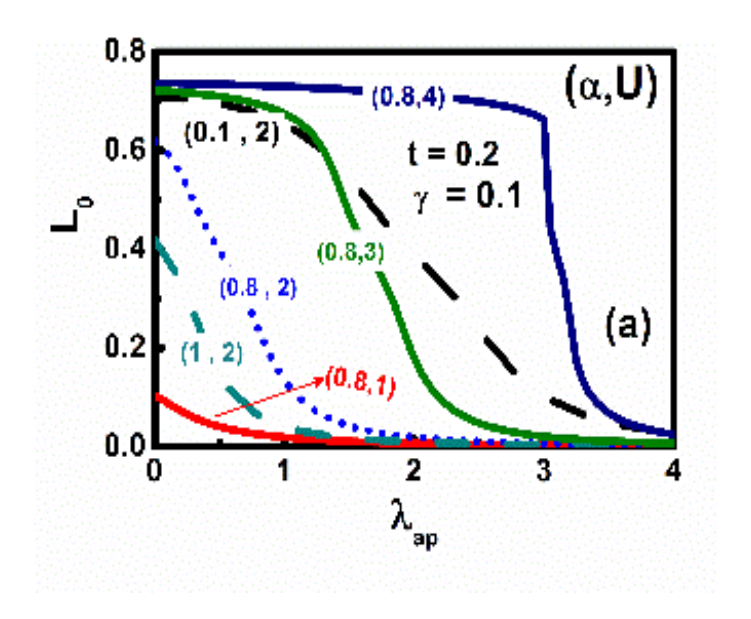
Fig. 10. (a) Eo versus g. (b) Eo versus U. (c) 3-dimensional plot of Eo on the a-U plane along with its contour graph.

Fig. 10(a) depicts the behaviour of von Neumann entropy (E_{θ}) (which gives the strength of quantum entanglement) with respect to g. The figures reveal that E_{ϑ} is symmetric for the case of harmonic lattice potential whereas for the anharmonic cases, E_{θ} is asymmetric. As g starts from the initial zero value, QE rises at a slow rate and reaches a peak and then drops off rather rapidly as g is further increased. location of the peak moves towards smaller g values, as the anharmonicity becomes stronger. The peak in the entanglement entropy suggests the existence of a metallic phase. Fig. 10(b) displays a peak in the quantum entanglement at some value of U. This reveals the existence of MP at the CDW-SDW crossover regime. The peak in the $(E_{\theta} - U)$ - curve moves towards a larger value of U with increasing anharmonicity. Fig. 10(c) illustrates the dimensional plot of E_{θ} with respect to U and α . The quantum entanglement exhibits a broad peak structure that satisfies the Mott's criteria for MP displayed in Fig. 5.

To understand the role of Gaussian anharmonicity on the quantum phase transition, we study in Figs. 11(a, b, c) the behaviour of L_0 , t_{eff}/t , and U_{eff} with respect to λ_{ap} . A cursory look at these graphs tells us that the values of the aforementioned quantities diminish as the

Gaussian anharmonicity is switched on. A closer inspection uncovers the following aspects.

(i) In Fig. 11(a), L_0 continues to be appreciable up to a specific value of λ_{ap} (which is higher for higher U) beyond which it sharply falls off to zero. The zero-value of L_0 implies the formation of bipolarons that are immobile and corresponds to the CDW state. Based on these observations, it can be inferred that a



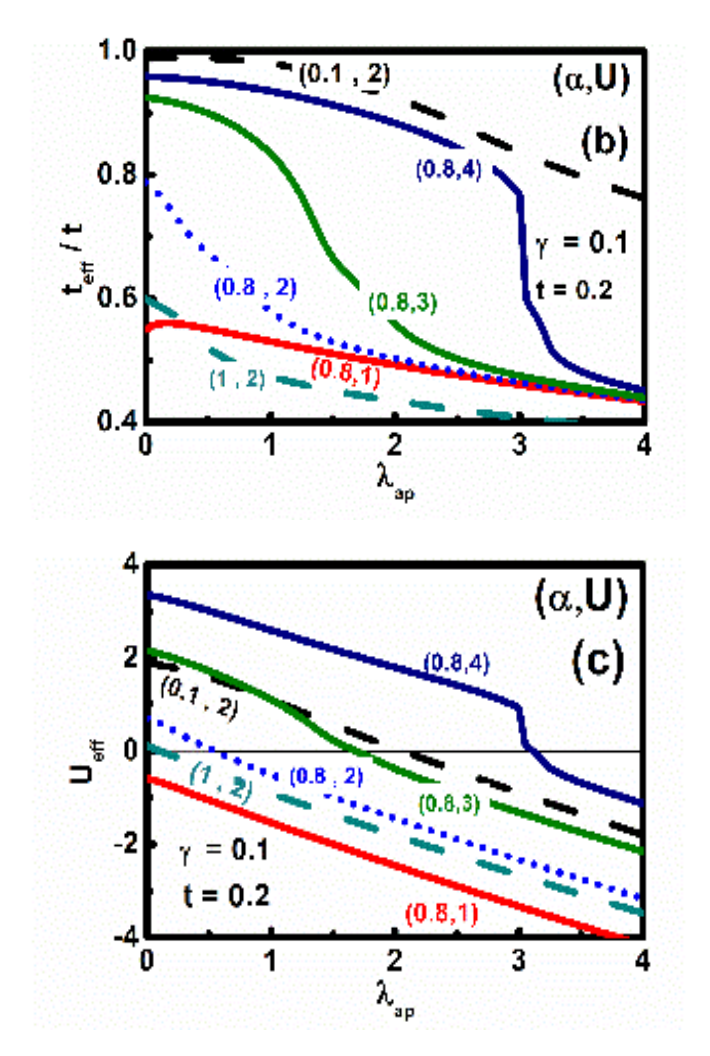


Fig. 11. (a) LSM (L₀) variation with λ_{ap} . (b) t_{eff}/t behaviour with λ_{ap} . (c) the behaviour of U_{eff} with λ_{ap} .

higher value of U increases the width of the SDW phase and reduces the width of MP. On the other hand, lower values of U broaden the MP. For a specified value of U, the e-p interaction suppresses L_0 (This is illustrated by the dotted curves in Fig. 11(a)).

- (ii) t_{eff}/t in Fig. 11(b) seems to exhibit similar traits as L_0 but it remains finite in the considered range of λ_{ap} . At lower values of anharmonicity, for a specified g, t_{eff}/t falls off quiet sharply with decreasing U. On the other hand, for a particular value of U, t_{eff}/t falls off rapidly with g at large g.
- (iii) One can see from Fig. 11(c) that for all sets of values of (U,α) , U_{eff} weakens with the rise in λ_{ap} and becomes negative at certain values of λ_{ap} . For a specified value of g, such values of λ_{ap} become smaller as U decreases. Similarly, for a specified value of U, as g is reduced, the value of anharmonicity at which U_{eff} becomes negative, increases. It is well known that the nature of the GS of a system is decided by the relative values of g and U. Here we have shown that the phonon anharmonicity also plays an important part in deciding the GS of the system by strengthening the e-p coupling.

2.5 Conclusion

In conclusion, we have studied in this chapter an Holstein-Hubbard chain with Gaussian phononic anharmonicity at half-filling. Successive application of a number of unitary transformations on the system Hamiltonian and many-phonon averaging have led to an effective Hubbard Hamiltonian which has been finally solved exactly by employing the Bethe ansatz method. The GS energy has been numerically computed by minimizing the variational energy with respect to the variational parameters. Using the Mott criterion, local spin moment, double occupancy and the von Newman entropy we further confirm the existence of a metallic phase at the SDW-CDW crossover region. We have also shown that the width of the metallic phase is broadened in the case of low anharmonicity.

References

- Y.H. Kim, A.J. Heeger, L. Acedo, G. Stucky and F. Wuld, *Phys. Rev. B*, **36**, no.13, pp. 7252-7255, (1987).
- B.K. Chakraverty, D. Feinberg, Z. Hang and M. Avignon, Sol. St. Com., 64, no.8, pp. 1147-1151 (1987).

Chapter 2: Metallicity in a Holstein-Hubbard.....

- 3. A.S. Alexandrov, *Phys. Rev. B*, **38**, no.1, pp. 925-927, (1988).
- 4. David Emin, *Phy. Rev. B*, **62**, no.13, pp. 1544-1547, (1989).
- 5. N.M. Plakida, *Physica C*, **162-164**, pp. 1341-1342, (1989).
- A.S. Alexandrov, *Physica C*, **158**, pp. 337-344, (1989).
- 7. Ashok Chatterjee and Shreekantha Sil, *Mod. Phys. Lett. B*, **6**, no.15, pp. 959-966 (1992).
- J. Konior, *Phys.Rev.B*, 47, no.21, pp. 14425-14433, (1993).
- 9. Shreekantha Sil and Bibhas Bhattacharyya, *Phys. Rev. B*, **54**,no.20, 14349-14354, (1996).
- 10. I.V. Sankar, Ashok Chatterjee, Eur. Phys. J. B, **87:154**, pp. 1-10, (2014).
- 11. K.A. Müller, *Physica C*, **341-348**, pp. 11-18, (2000).
- 12. Yasutami Takada, *J. Phys. Soc. Jap.*, **65**, no.6, pp. 1544-1547(1996).
- 13. J. E. Hirsch and E. Fradkin *Phy. Rev. Let.* **49** 6 402-405 (1982).
- 14. Yasutami Takada and Ashok Chatterjee, *Phys. Rev. B*, **67**, pp. 081102(R) (1-4), (2003).
- 15. Ashok Chatterjee and Yasutami Takada, *J. Phys. Soc. Jap.*, **73**, no.4, pp. 964-969, (2004).

- 16. P.M. Krishna and Ashok Chatterjee, *Physica C*, **457**, pp. 55-59, (2007).
- 17. Ashok Chatterjee, *Adv. Con. Matt. Phys.*, **2010**, pp. 350787 (1-14), (2010).
- 18. H. Fehske, G. Hager and E. Jeckelmann, *Eur. Phys. Lett.*, **84**, pp. 57001 (1-6), (2008).
- 19. R.T. Clay and R.P. Hardikar, *Phys. Rev. Lett.*, **95**, pp. 096401 (1-4), (2005).
- 20. R.P. Hardikar and R.T. Clay, *Phys. Rev. B.* **75**, pp. 245103 (1-10), (2007).
- 21. R.T. Clay, A.W. Sandvik and D.K. Campbell, *Phys. Rev. B.* **59**, no. 7, pp. 4665-4679, (1999).
- 22. S. Ejima and H. Fehske, *Eur. Phys. Lett.* **87**, pp. 27001 (1-7), (2009).
- 23. S. Ejima and H. Fehske, *J. Phys.: Conf. Ser.*, 200, pp. 012031 (1-4), (2010).
- 24. Ka-Ming Tam, S.-W. Tsai and D.K. Campbell, *Phys. Rev. B.* **84**, pp. 165123 (1-6), (2011).
- 25. M. Hohenadler and F.F. Assaad, *Phys. Rev. B.* **87**, pp. 075149 (1-10), (2013).
- Ka-Ming Tam, S.-W. Tsai and D.K. Campbell, *Phys. Rev. B.* 89, pp. 014513 (1-7), (2014).
- H. Mosadeq and R. Asgari, *Phys. Rev. B.* 91, pp. 085126 (1-9), (2015).

Chapter 2: Metallicity in a Holstein-Hubbard.....

- J. Greitmann, S. Hesselmann, S. Wessel, F.F. Assaad and M. Hohenadler, *Phys. Rev. B.* 92, pp. 245132 (1-16), (2015).
- 29. I.V. Sankar and Ashok Chatterjee, *Physica B.* **489**, pp. 17-22, (2016).
- 30. E.H. Lieb and F.Y. Wu, *Phys. Rev. Lett.* **20**, no. 25, pp. 1445-1448, (1968); ibid. *physica A.* **321**, pp. 1-27, (2003).
- 31. A. Einstein, B. Podolsky and N. Rose, *Phys. Rev.* **47**, pp. 777-780, (1935).
- 32. D. Bohm, Quantum theory, Constable and Company, London, (1954).
- 33. A.Aspect, J. Dalibard and G. Roger, *Phys. Rev. Lett.* **49**, no. 25, pp. 1804-1807, (1982); A. Peres, Quantum Theory: concepts and Methods, Kluwer academic publishers, Dordrecht, (1993).
- 34. M. A. Nielsen and I. L. Chuang, Quantum computation and Quantum Information, Cambridge University press, Cambridge, (2000).
- 35. S. Sachdev, Quantum Phase Transitions, Cambridge University press, (1999).
- A. Osterloh, L. Amio, G. Fali and R. Fazio, *Nature* 416, no. 11, 608-610, (2002); L. –A Wu, M.S. Sarandy and D.A. Lindar, *Phys. Rev. Lett.*

Phase transitions in one-Dimensional Hol.....

93, pp. 250404 (1-4), (2004); S.J. Gu, S.S. Deng, Y.Q.Li and H.Q. Lin, *Phy. Rev. Lett.* **93**, pp. 086402 (1-4), (2004).

Chapter 3

Persistent Currents in the 1D Holstein-Hubbard ring by Bethe-ansatz approach

3.1 Introduction

The subject of mesoscopic rings has received significant attention from both theorists and experimentalists. One of the most important reasons for this is their property of sustaining persistent currents. Persistent charge and spin current can be generated in mesoscopic rings threaded by magnetic flux.

Both experimental [1-11] and theoretical [12-17] studies have been carried out on PC in a mesoscopic quantum ring (QR) over the last three decades. Another intriguing feature of the PC is that it also depends on the spin dependence of the magnetic flux applied to the mesoscopic ring. The subject of quantum computers [18] has emerged as a very exciting area in recent times and quantum technology is expected to play a crucial role in future in which

QRs will have major applications. The Hubbard Model, which admits an exact solution in one dimension, is the most convenient theoretical model to study such quantum rings with interactions. Such type of rings shall be referred to as the Hubbard QR (HQR). Finite HQR has been studied by Wei et al. [19] with the help the Bethe-ansatz method to determine the persistent charge current (PCC) as well as the persistent spin current (PSC) in it. But the effect of *e-p* interaction has not been incorporated in this study. To explore the combined effects of *e-e* and *e-p* interactions one needs to examine the Holstein-Hubbard (HH) model for QR (HHQR). Sankar et al. [20] have made an attempt to calculate PC in a one-dimensional (1D) HHQR using the mean-field approximation (MFA).

The present chapter is devoted to the investigation of the *e-p* interaction effects on PCC and PSC in a finite HHQR by exploiting the BA technique which gives an exact solution for the 1D Hubbard model. We also study the dependence of PCC and PSC on the size of HHQR. Finally, the local spin moment, double occupancy and entanglement entropy are calculated to study the quantum phase transitions in the system.

3.2 Hamiltonian and the model

The Hamiltonian for the HHQR system threaded by the AB flux can be written as

$$H = H_{el} + H_{ph} + H_{el-ph}$$
, (3.1)

with

$$H_{el} = -t \sum_{\langle ij \rangle \sigma} e^{\pm i \left(\frac{\phi_{\sigma}}{L}\right)} c_{i\sigma}^{\dagger} c_{j\sigma} + U \sum_{i} n_{i\uparrow} n_{i\downarrow}, (3.1a)$$

$$H_{ph} = \hbar \omega_0 \sum_{i} b_i^{\dagger} b_i , \qquad (3.1b)$$

$$H_{ep} = g_0 \sum_{i\sigma} n_{i\sigma} (b_i^{\dagger} + b_i)$$

$$+ g_1 \sum_{i\sigma\delta} n_{i\sigma} (b_{i+\delta}^{\dagger} + b_{i+\delta}), \quad (3.1c)$$

In the above equations, $c_{i\sigma}^{\dagger}$ ($c_{i\sigma}$) represents the electron operator that creates (annihilates) an electron at site i, σ representing the electron spin which has two possibilities ($\sigma = \uparrow, \downarrow$), the bare nearest-neighbour (NN) hopping parameter t is modified by the Peierl's phase factor, $e^{\pm i(\phi_{\sigma}/L)}$ (the direction of hopping

deciding the sign), ϕ_{σ} denoting the spin-dependent flux $(\sigma = \uparrow, \downarrow)$ (in units of flux quantum $\phi_0 = hc/e$), $n_{i\sigma}$ (= $c_{i\sigma}^{\dagger}c_{i\sigma}$) is the number operator for an electron of spin σ at site i, U stands for the on-site e-e Coulomb interaction energy, b_i^{\dagger} (b_i) stands for the operator that creates (annihilates) a phonon at site, ω_0 refers to the dispersionless frequency and g_0 and g_1 denote respectively the onsite and NN e-p interaction strengths. Another important parameter which is related to the applied magnetic field is the spin-dependent vector potential (A_{σ}) . This is written as: $A_{\sigma} = (hc/e) \phi_{\sigma}/L$

3.3 Formulation

3.3.1 GS Energy

As a first step, we perform the conventional Lang-Firsov canonical transformation with the following generator:

$$R = \frac{g_0}{\hbar\omega_0} \sum_{i} n_{i\sigma} (b_i^{\dagger} - b_i),$$

$$+ \frac{g_1}{\hbar\omega_0} \sum_{i\delta} n_{i\sigma} (b_{i+\delta}^{\dagger} - b_{i+\delta}). \tag{3.2}$$

As a result of the above transformation, the Hamiltonian (3.1) is transformed as follows:

$$\widetilde{H} = e^R H e^{-R} \tag{3.3}$$

$$\begin{split} \widetilde{H} &= -te^{i\phi} \sum_{i\delta\sigma} C_{i\sigma}^{\dagger} C_{i+\delta,\sigma} \\ &\times \exp\left(\frac{g_0'}{\omega_0} (b_i^+ - b_i) - \frac{g_0'}{\omega_0} (b_{i+\delta}^{\dagger} - b_{i+\delta}) \right. \\ &\quad + \frac{g_1'}{\omega_0} \sum_{\delta'} (b_{i+\delta'}^{\dagger} - b_{i+\delta'}) \\ &\quad - \frac{g_1'}{\omega_0} \sum_{\delta'} (b_{i+\delta+\delta'}^{\dagger} - b_{i+\delta+\delta'}) \right) \\ &\quad + U \sum_{i} n_i n_i + \omega_0 \sum_{i} b_i^{\dagger} b_i - g_0' \sum_{\sigma} n_{i\sigma} (b_i^+ + b_i) \\ &\quad - g_1' \sum_{\delta'\sigma} n_{i+\delta',\sigma} (b_i^{\dagger} + b_i) + \frac{(g_0')^2}{\omega_0} \sum_{\sigma\sigma'} n_{i\sigma} n_{i\sigma'} \\ &\quad + \frac{(g_1')^2}{\omega_0} \sum_{\delta'\delta''\sigma\sigma'} n_{i+\delta',\sigma} n_{i+\delta'',\sigma'} \\ &\quad + g_0 \sum_{i\sigma} n_{i\sigma} (b_i^{\dagger} + b_i) \\ &\quad + \frac{g_0' g_1'}{\omega_0} \sum_{\delta'\sigma\sigma'} (n_{i+\delta',\sigma} n_{i\sigma'} + n_{i\sigma} n_{i+\delta',\sigma'}) \end{split}$$

$$-\frac{2gg'}{\omega_0} \sum_{i\sigma\sigma'} n_{i\sigma} n_{i\sigma'}$$

$$-\frac{2g_0g'_1}{\omega_0} \sum_{i\delta'\sigma\sigma'} n_{i\sigma} n_{i+\delta'\sigma'}$$

$$-\frac{2g_1g'_0}{\omega_0} \sum_{i\delta\sigma\sigma'} n_{i\sigma} n_{i+\delta,\sigma'}$$

$$-\frac{2g_1g'_1}{\omega_0} \sum_{i\delta\delta'\sigma\sigma'} n_{i\sigma} n_{i+\delta+\delta',\sigma'}$$

$$+g_1 \sum_{i\delta\sigma} n_{i\sigma} (b_{i+\delta}^{\dagger} + b_{i+\delta}). \tag{3.4}$$

The total wave function $|\Psi\rangle$ is now written as the product of the state $|\Psi_e\rangle$ which is a function of electron variables and the state $|\Psi_p\rangle$ which contains phonon variables i. e.,

$$|\Psi\rangle = |\Psi_p\rangle|\Psi_e\rangle. \tag{3.5}$$

The Energy is then given by:

$$E = \langle \Psi | \widetilde{H} | \Psi \rangle$$
$$= \langle \Psi_e | \langle \Psi_p | \widetilde{H} | \Psi_p \rangle | \Psi_e \rangle$$

$$= \langle \Psi_e | H_{eff} | \Psi_e \rangle, \tag{3.6}$$

where

$$H_{eff} = \langle \Psi_p | \widetilde{H} | \Psi_p \rangle \tag{3.7}$$

For the averaging phonon state, we consider the zero-phonon state: $|\Psi_p\rangle=|0\rangle=\prod_i|0_i\rangle$ where $c_i|0_i\rangle=0$. Then H_{eff} reads

$$H_{eff} = -\varepsilon_{eff} \sum_{i\sigma} n_{i\sigma} - t_{eff} \sum_{i\delta\sigma} e^{\pm i\frac{\phi_{\sigma}}{L}} c_{i\sigma}^{\dagger} c_{i+\delta,\sigma}$$

$$+ U_{eff} \sum_{i} n_{i\uparrow} n_{i\downarrow}, \qquad (3.8)$$

with

$$\varepsilon_{eff} = -\frac{(g_0^2 + zg_1^2)}{\hbar\omega_0},\tag{3.8 a}$$

$$t_{eff} = te^{-((g_0 - g_1)^2 + (z - 1)g_0^2)/(\hbar\omega_0)^2},$$
 (3.8 b)

$$U_{eff} = U - 2(g_0^2 - zg_1^{2'})/\hbar\omega_0.$$
 (3.8 c)

We set $\hbar = 1 = \omega_0$ from here onwards. The effective Hamiltonian (3.8) can be solved by using the nested Bethe-Ansatz method. Application of the Bethe ansatz method to the 1D Hubbard model [19] gives rise to a set of following transcendental equations.

$$e^{ik_jL} = e^{i\phi_{\uparrow}} \prod_{\beta=1}^{M} \frac{\sin k_j - \Lambda_{\beta} + iu}{\sin k_j - \Lambda_{\beta} - iu}, \qquad (3.9a)$$

$$e^{i(\phi_{\downarrow} - \phi_{\uparrow})} \prod_{j=1}^{N_c} \frac{\Lambda_{\alpha} - \sin k_j + iu}{\Lambda_{\alpha} - \sin k_j - iu}$$
$$= - \prod_{\beta=1}^{M} \frac{\Lambda_{\alpha} - \Lambda_{\beta} + iu}{\Lambda_{\alpha} - \Lambda_{\beta} - iu}$$
(3.9b)

where j=1,2,3,....N, $\alpha=1,2,3,....M$, $u=U_{eff}/4t_{eff}$, N being the total number of fermions and M the number of spin-down fermions. As a result, we get two sets of variables namely the quasi-

momentum $\{k_j\}$ and the spin rapidities $\{\Lambda_{\alpha}\}$. The values of these two sets of variables can be obtained by using an iterative numerical method to solve the above mentioned coupled transcendental equations (3.9a) and (3.9b). Eventually, the energy eigenvalues can be expressed as follows:

$$\epsilon(\phi) = -\varepsilon_{eff}N - 2\sum_{j=1}^{N} \cos k_j + \frac{\left(U_{eff} - \left|U_{eff}\right|\right)}{4}$$
(3.10)

The energy per site is given by

$$E(\phi) = \frac{\epsilon(\phi)}{N} \tag{3.11}$$

3.3.2. Persistent Charge current and Persistent Spin Current

In a usual electronic system, there exists a conventional current which is the charge current. In QR, the current can be persistent that means it can stay in the system for a long time without any external power supply. Recently, another kind of current has been found in a quantum mesoscopic ring which is PSC. This current is due to the change in the magnetization of the system caused by the fluctuations in the spin. In the present chapter we consider both spin up and spin down

electrons with two different and independent parameters ϕ_{\uparrow} and ϕ_{\downarrow} . We use these parameters ϕ_{\uparrow} and ϕ_{\downarrow} in (3.9a) and (3.9b) to calculate PCC and PSC. To compute PCC (I_c), we consider $\phi_{\uparrow} = \phi_{\downarrow} = \phi$. Once we estimate the GS energy of the system, we can calculate PCC without any difficulty by employing the Hellmann-Feynman theorem [19] as follows:

$$I_C = -\frac{\partial E(\phi)}{\partial \phi} \ . \tag{3.12}$$

In the same way, using the condition: $-\phi_{\uparrow} = \phi_{\downarrow} = \phi$, PSC can be computed from the following equation:

$$I_{S} = -\frac{1}{2} \frac{\partial E(\phi)}{\partial \phi} \,. \tag{3.13}$$

3.4. Results and Discussion

3.4.1 GS energy

For convenience in numerical computation, we set t=1 in this work. We study four cases: (i) $\langle n \rangle = 1/2$, (ii) $\langle n \rangle = 1/3$, and $\langle n \rangle = 1/4$, where $\langle n \rangle$ indicates the average number of electrons per site.

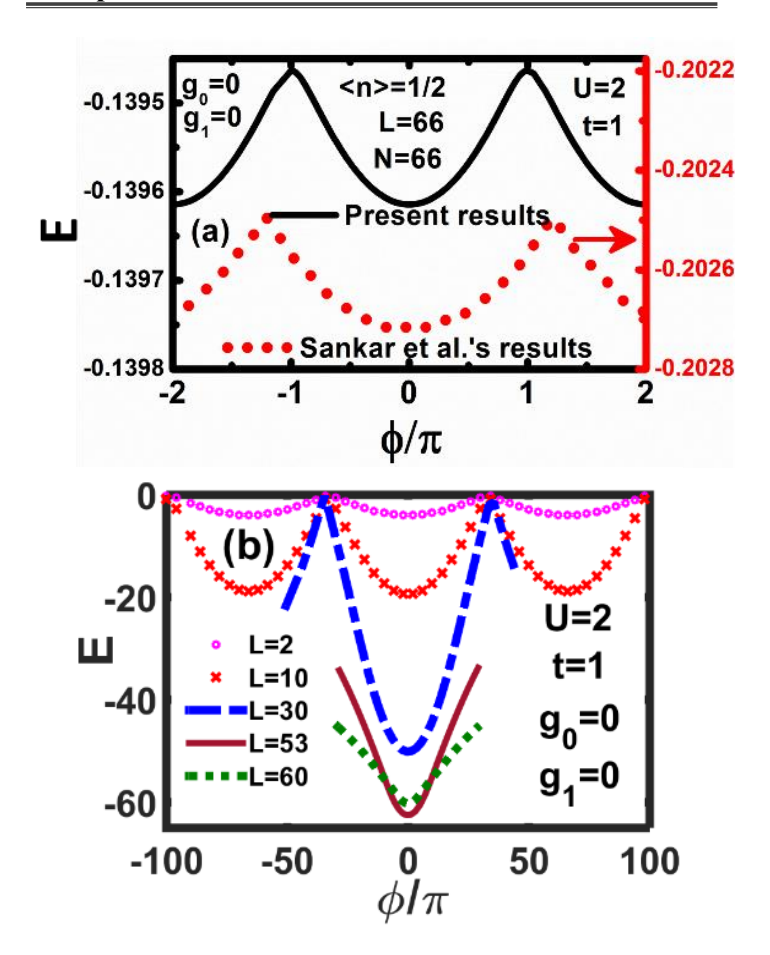


Fig. 1 GS energy per site vs. magnetic flux ϕ (a) for half filling, $\langle n \rangle = 1/2$, (b) for away from half filling $\langle n \rangle = 2/5$.

The transcendental equation (3.9a) and (3.9b) are first solved and then the energy per site $(E = \epsilon/N)$ is determined using Eq. (3.10). This energy is plotted in

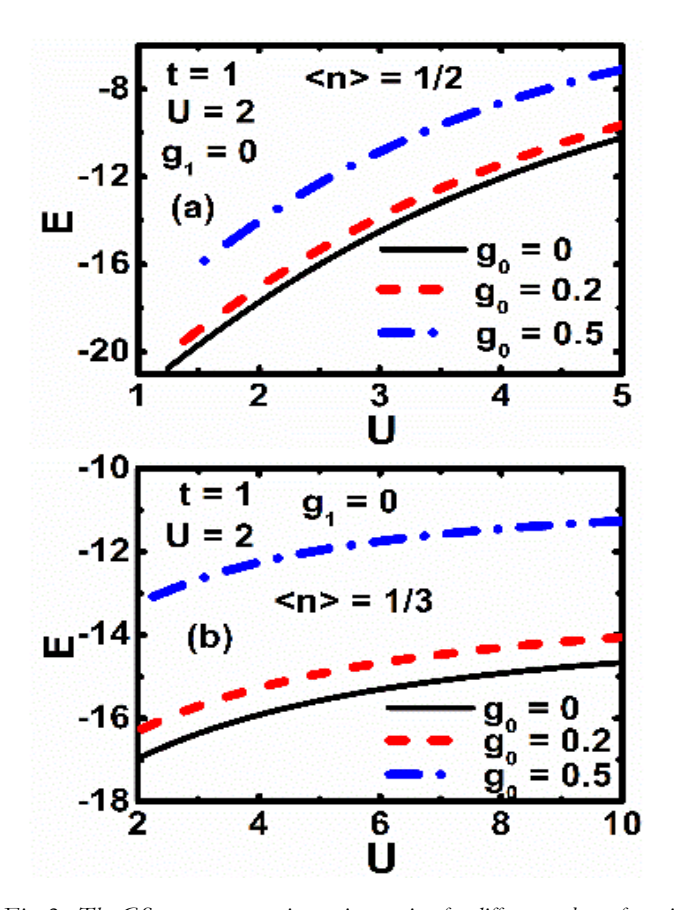


Fig. 2. The GS energy vs. on-site e-e interaction for different values of on-site e-p interactions for L=66. (a) At half-filling (< n> = 1/2), (b) at away from half filling (< n> = 1/3).

Fig. 1(a) as a function of the magnetic flux (ϕ) at half-filling for the system size L=66 and with U=2 in

the absence of e-p interactions i. e., for $g_0 = 0 = g_1$. We would also like to compare the behaviour of E versus U at half-filling with that at away from half-filling. Fig.2 shows this comparison.

As stated above, E versus U is plotted in Fig. 2(a) for different values of g_0 at half filling, while the same for $\langle n \rangle = 1/3$ is plotted in Fig. 2(b). One can see that compared to the half-filled case, the energy in the case of away from half filling varies much slowly with respect to U. Consequently, while in general, the energy in the half-filled case is lower at small U, in the away from half-filled case, it becomes lower at large U.

3.4.2 Persistent charge current (PCC)

(a) Flux dependence of PCC

As visible from Eq. (3.12), PCC (I_c) also exhibits a periodic variation with the magnetic flux ϕ like the GS energy. Fig. 3(a) depicts the behaviour of I_c with respect to ϕ for L = 66, $\langle n \rangle$ = 1/2, U = 2 and a set of values of g_0 . The behavior at away from half-filling is depicted in Fig. 3(b). Two electrons normally repel each other and when U is large, the GS is a polaronic Mott antiferromagnetic Mott spin-density-wave

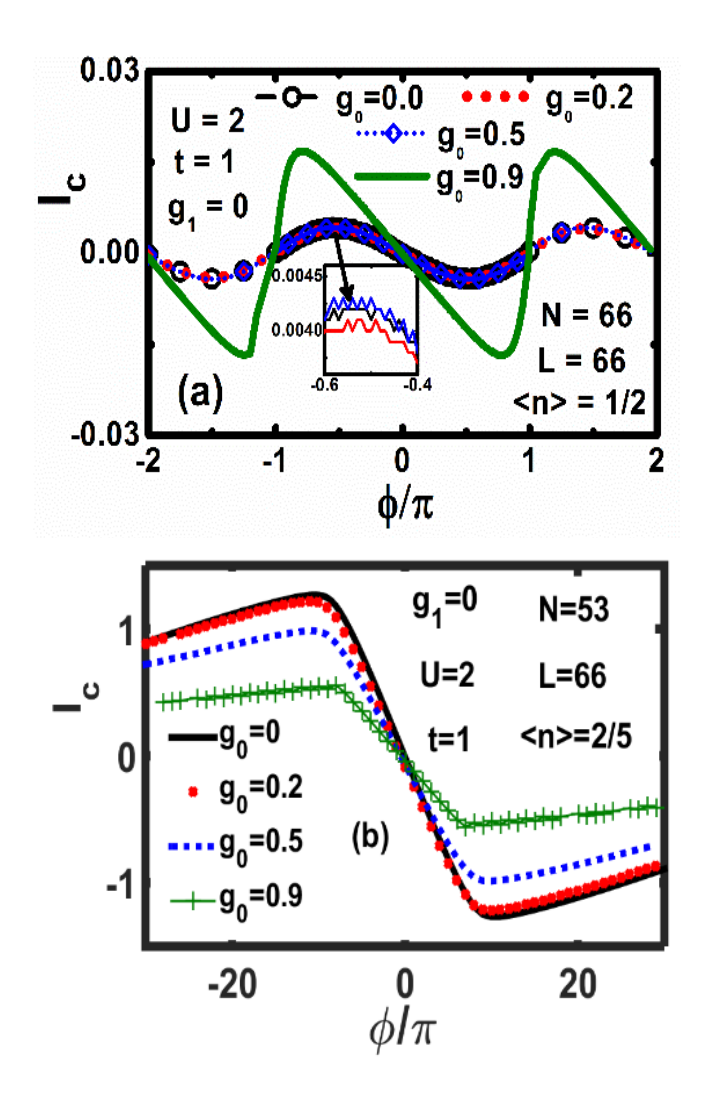


Fig. 3 PCC I_c vs magnetic flux ϕ for different values of g_0 with L=66 at : (a) < n > = 1/2, (b) < n > = 2/5.

(SDW) insulator, whereas two electrons can form an onsite bound pair in the case of large e-p interaction, and then the GS is a bipolaronic Peierls chargedensity-wave (CDW) insulator. It can be noted from Fig. 3(a) that in the case of half filling, the magnetic flux brings in a periodic change in the phase which in turn gives rise to a sinusoidal behaviour in I_c . One can see from the inset of Fig. 3(b) that when when g_0 increases from zero to 0.5, I_c does not show any perceptible change. But a large change happens when g_0 approaches 0.9. Though the behaviour is still periodic, it does not vary sinusoidally. But now the current shows a larger value. The increase in the current may be caused by the motion of correlated electron-pairs which are bipolarons. This is observed only in the case of half-filling. We find from Fig. 3(b) that in the case of away from half-filling also, I_c vs ϕ - curve is periodic. In this case, the current has a higher magnitude than that of the half-filling case. This may be because in the case of away from half filling, more states are available to the carriers. In a previously reported work [19], I_c exhibits an oscillatory behavior in both half-filled and non-half-filled cases.

In another recent work [20], the researchers have chosen to work with the peak value of PCC (Fig. 3(a)) with the corresponding magnetic flux. One can work with any non-zero value of ϕ because the physical analysis is not affected by the choice of ϕ as long as ϕ

is nonzero. Here we will work with $\phi = -0.8 \,\pi$ (a value close to the one corresponding to the peak in PCC).

(b) PCC and Coulomb Correlation

The behaviour of I_c as a function of U in the halffilled case is depicted in Fig. 4 with L = 66 and for different values of g_0 . I_c is found to be large at low values of U. Therefore, the system will be expected to show a conducting behaviour in this region. With increasing U, I_c undergoes a rapid decrease and falls off to zero at some U value. Thus, beyond this critical U, the system will be expected to behave as an insulator. At low U, I_c turns out to be large for large g_0 while at large U, I_c does not seem to have any dependence on g_0 . These results can be justified on physical grounds. The *e-p* interaction considerable effect on PC at low U, while at large U, PC does not have any dependence on e-p interaction. Therefore, we conclude here that certain windows of ee and e-p couplings are favourable for the occurrence of a metallic phase.

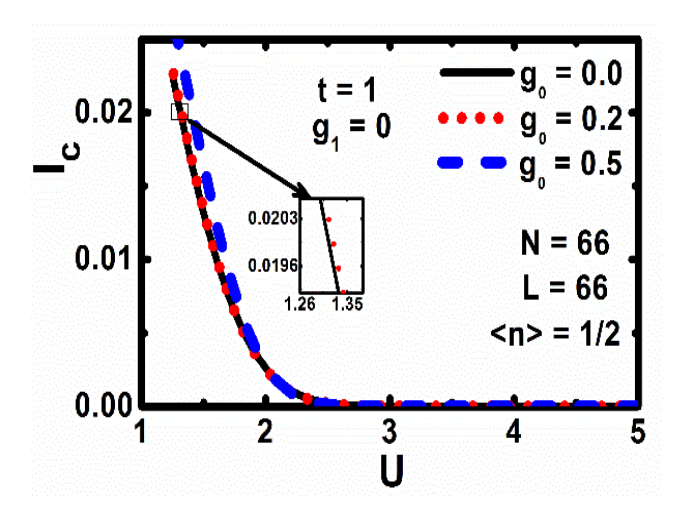


Fig. 4 I_c vs U for different values of g_0 at half filling.

It would be interesting to have results on functional dependence of I_c on U (for different g_0 values). In order to examine this aspect, $\ln I_c$ is plotted with respect to U^2 at half filling in Fig. 5 and an appropriate expression is obtained by fitting the data. Wei et al. [20] have already made such an attempt. Our results for $g_0=0$ are in agreement with their results. We find that for $g_0=0-0.5$, the behaviour can be approximately fitted to the equation: $I_c=I_{c0}\exp(-U^2/\xi)$, where $\sqrt{\xi}$ gives the energy scale over which the persistent current vanishes. It is found that $\xi=1$. For $g_0=0.9$, however, the data fit the equation: $I_c=I_{c0}\exp(-U/\xi)$.

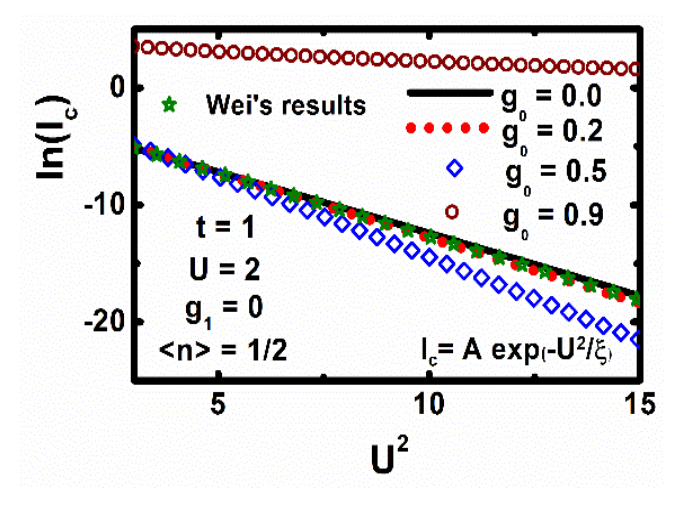
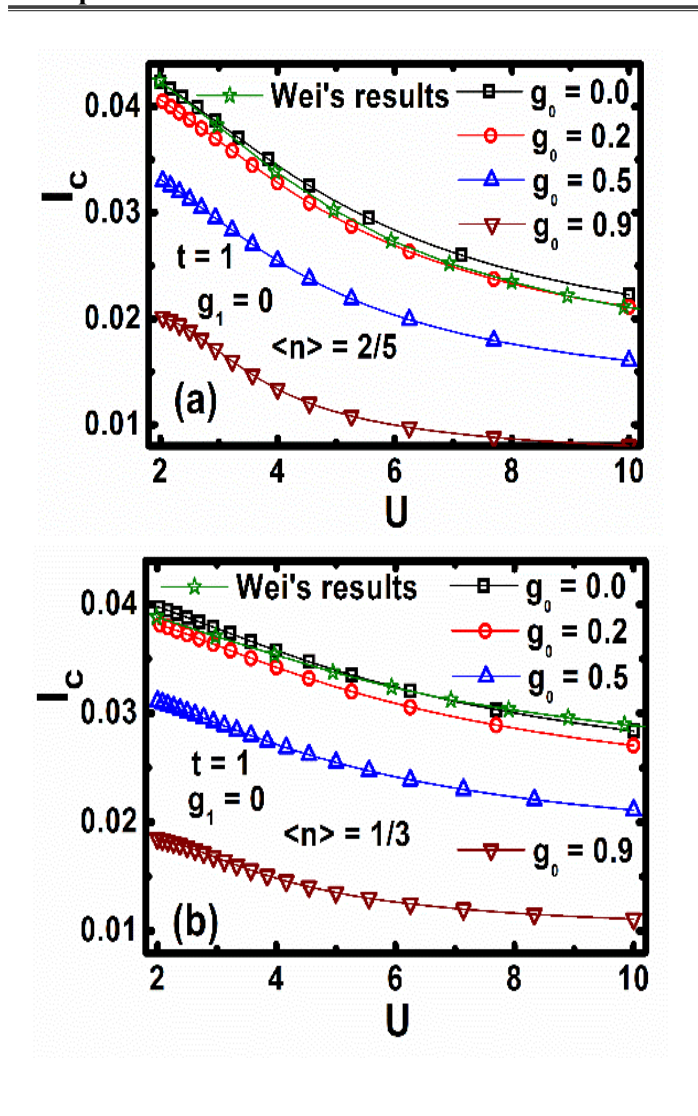


Fig. 5 $\ln I_c \text{ vs } U^2$ at half-filling (<n> = 1/2) for $g_0 = 0, 0.2, 0.5, 0.9$.

The results for I_c vs U for $\langle n \rangle < 1/2$ are depicted in Figs. 6 (a-c). The interesting point to note in the results in these cases is that, I_c never goes to zero. Consequently, one can conclude that a system with less than half filling would always be in a metallic state irrespective of the value of U and one would not expect such a system to show any metal-insulator transition. To get a deeper understanding of the metallic behavior at away from half filling, we again



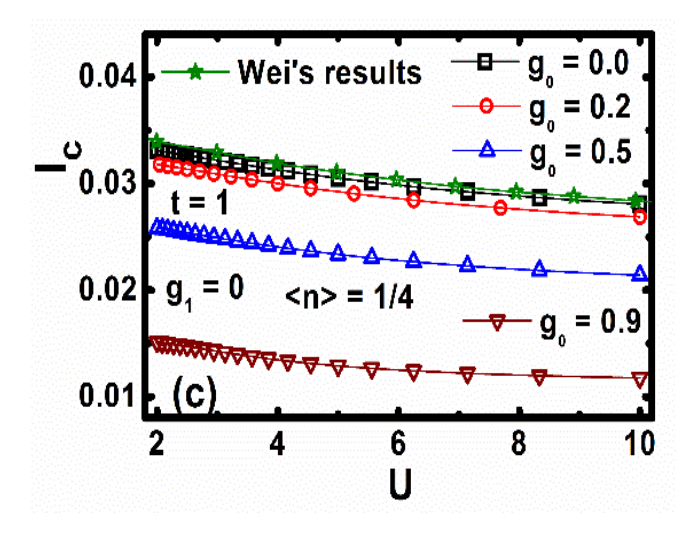


Fig. 6 I_c vs U at away from half-filling for $g_0 = 0, 0.2, 0.5$, 0.9. (a) < n > = 2/5, (b) < n > = 1/3 and (c) < n > = 1/4

attempt to fit the I_c-U data with an appropriate expression. We find that the results can be fitted to the equation: $I_c = A \exp(-U^m/\xi) + B$, where (A+B) is clearly the value of I_c at U=0 and B the value of I_c at large U. Comparison of the expressions for I_c for the half-filling and non-half-filling cases clearly shows that because of the presence of the non-zero parameter B in the latter case, I_c never vanishes in this case and consequently in this case, the system always remains in the metallic state. We find that $\xi > 1$ and m < 2 in the non-half-filled cases More

specifically, ξ turns out to be around 10 and m decreases from 2, as < n > decreases from 1/2. For example, m = 1.5 for < n > = 2/5, m = 1.4 for < n > = 1/3, and m = 1.3 for < n > = 1/4.

(c) PCC and e-p interactions

Fig. 7 illustrates how I_c varies with g_0 for $\langle n \rangle$ = 1/2 for a few values of U. In Fig. 7(a), I_c vs g_0 – graph is shown for a few values of U with $g_1 = 0$ and $g_1 = 0.2$. I_c seems to be symmetric around $g_0 = 0$. For U = 0, I_c shows a broad maximum around $g_0 =$ 0, which indicates the existence of a metallic phase. As g_0 is increased, I_c drops and ultimately falls off to zero at some value of g_0 . Beyond this critical value of g_0 , the system will be naturally in an insulating phase. For U > 0, however, I_c shows a different behaviour. As g_0 is increased from zero, it first rises with g_0 , reaches a maximum at a certain value of g_0 and then drops rather rapidly but smoothly to zero. It has been observed that as U is increased, I_c also decreases and its maximum moves to a higher value of g_0 . For a sufficiently large value of U, I_c continues to remain zero up to a large value of g_0 and

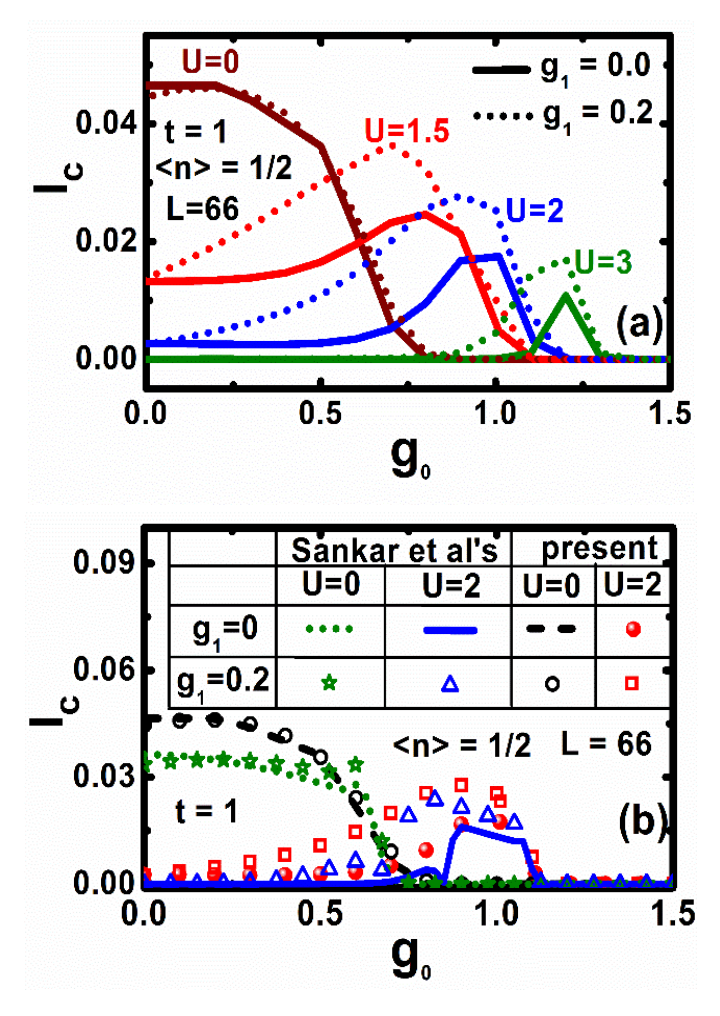
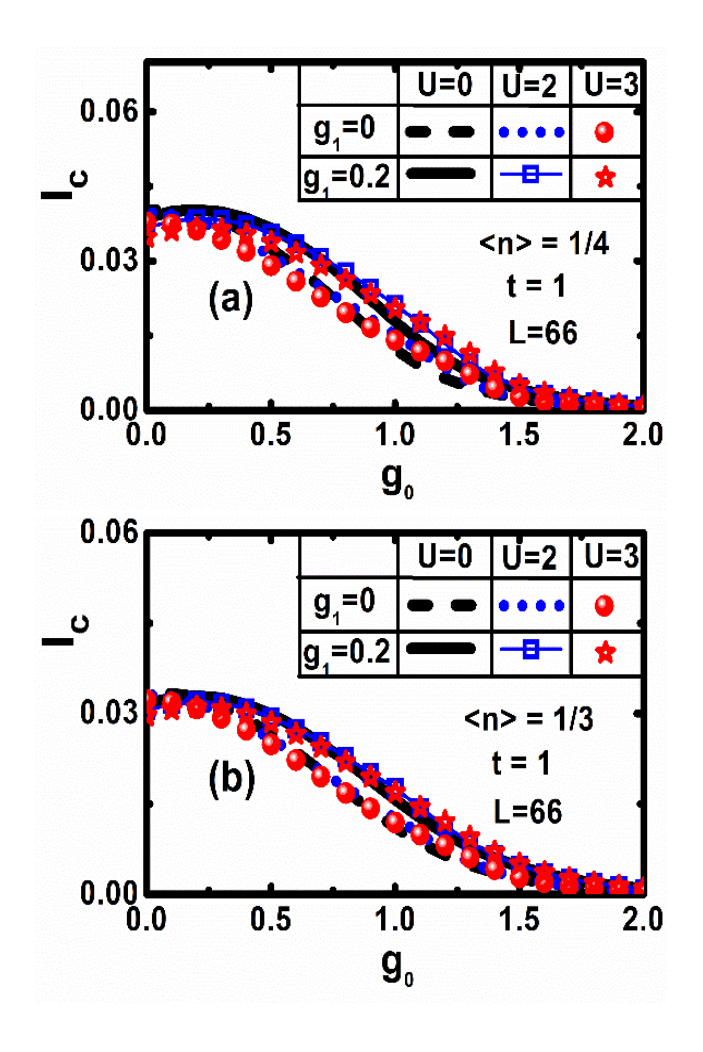


Fig. 7 (a) I_c versus g_0 ; (b) I_c versus g_0 . The results of Sankar. et al. [21] are also shown for comparison.

then exhibits a small maximum and finally again falls off to zero. Fig. 7(b) shows the comparison of our present results with those obtained by Sankar et el. by invoking the mean field approximation [20]. In contrast to the mean theory of Sankar et al. [20] which shows a kink-like behavior in I_c before its rapid fall to zero, the present results do not indicate any sudden transition in the system. This leads to the conclusion that at low values of g_0 and U, the system would like to be in a metallic state. The results with respect to g_1 and U lead us to similar conclusion (not shown here).

Figs. 8 (a-c) depict the behavior of I_c with respect to g_0 for a few values of U and g_1 for $\langle n \rangle \neq 1/2$. Fig. 8(a) shows the manner in which I_c behaves with g_0 for $\langle n \rangle = 1/4$, while Figs. 8(b) and 8(c) display the case for $\langle n \rangle = 1/3$ and $\langle n \rangle = 2/5$, respectively. Unlike in the case of $\langle n \rangle = 1/2$, I_c now turns out to be a slowly decreasing function of g_0 . For $g_1 = 0$, I_c seems to have, in general, a maximum at $g_0 = 0$. As g_1 increases, the maximum of I_c moves in the direction of the higher values of g_0 , while U appears to reduce the height of the maximum. Furthermore, for intermediate values of g_0 , I_c is enhanced by g_1 .



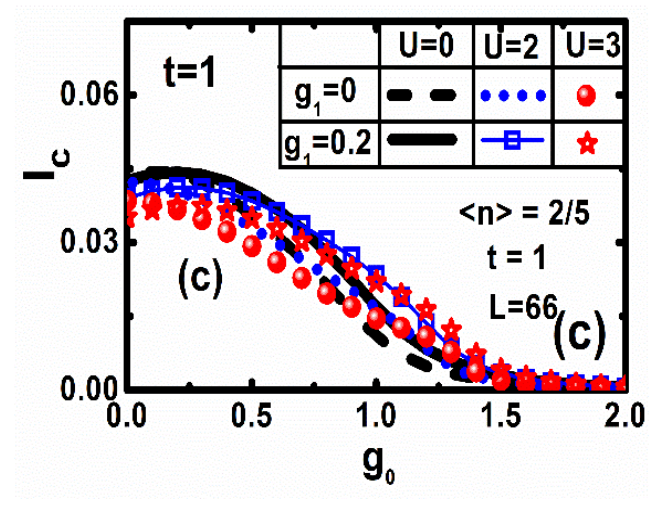
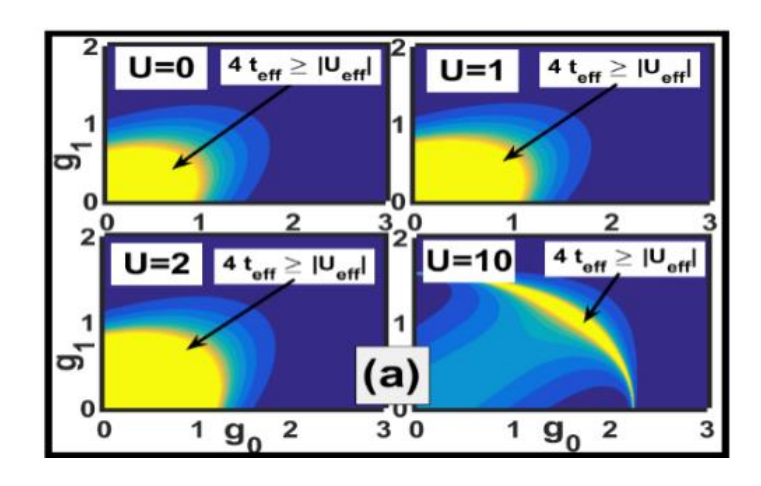
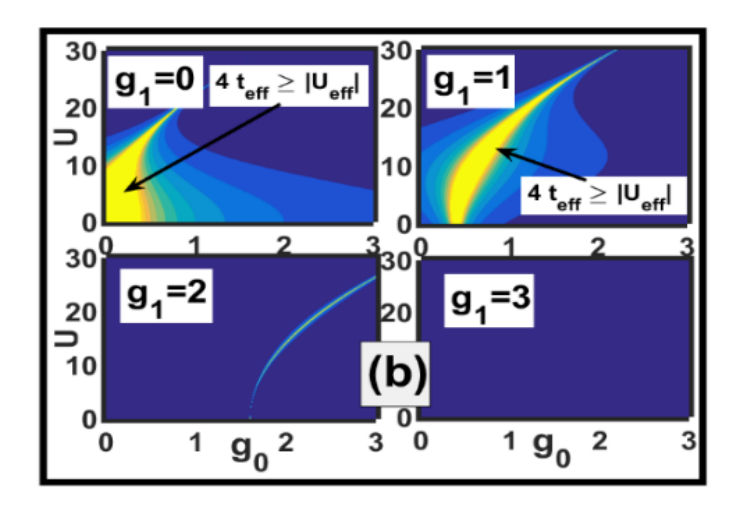


Fig. 8 PCC vs g_0 for different combination of U and g_1 with L=66 at away from half—filling ((a) $< n > = \frac{1}{4}$, (b) $< n > = \frac{1}{3}$ and (c) $< n > = \frac{2}{5}$.

(d) PCC and Phase transitions

The condition: $4t_{eff} \ge |U_{eff}|$ is a crucial criterion that is satisfied by a metallic phase. It is referred to as the Mott criterion or the metallicity criterion in this thesis and we make use of it to determine the metalinsulator transition from Eqs. (2b) and (2c) for different range U, g_0 and g_1 . In the yellow regions in Fig. 9, the condition of metallicity is satisfied and the





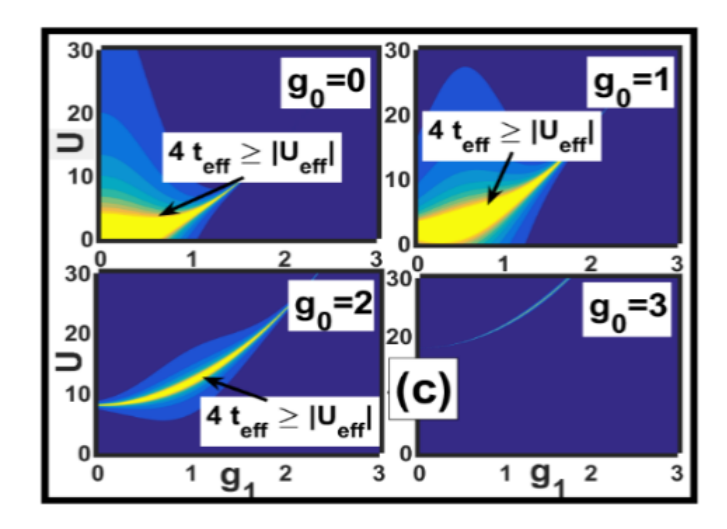


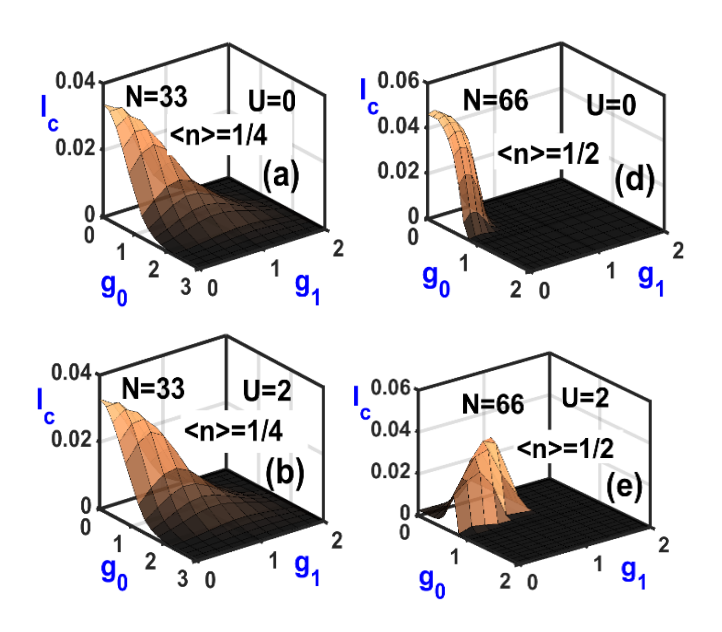
Fig. 9 Metallicity criterion ($4t_{eff} \ge |U_{eff}|$): (a) in the (g_0, g_1) plane for U = 0, U = 1, U = 2 and U = 10; (b) in the (g_0, U) plane for $g_1 = 0$, $g_1 = 1$, $g_1 = 2$ and $g_1 = 3$; (c) in the (g_1, U) plane for $g_0 = 0$, $g_0 = 1$, $g_0 = 2$, $g_0 = 3$

blue areas indicate the insulating regions. In the four panels in Fig. 9(a), the metallic phases are shown in the $(g_0 - g_1)$ -plane for U = 0, 1, 2 and 10. For U = 0, the metallic criterion is satisfied for $g_0 < 1$ and $g_1 < 1$. The metallic phase spreads out as U is increased from 0 to 2. However, as U is increased further, the metallicity condition is satisfied at larger values of g_0 and g_1 . Consequently, the metallic phase becomes thinner. In Fig. 9(b), the criterion of metallicity is examined in the (U, g_0) – plane for a few values of

 g_1 . As g_1 is increased, the metallic region shifts towards the higher g_0 - values. Finally at some value of g_1 , the metallic phase ceases to exist. Similarly, we study the metallicity criterion in the (U,g_1) - plane for a few values of g_0 . This is displayed in Fig. 9(c). It is observed from the figure that as we increase g_1 , eventually the metallic phase dies out completely. The aforementioned graphs can be used to find the ranges of U, g_0 and g_1 which will provide a metallic phase that can allow a persistent current to flow.

In Fig. 10, PCC is plotted with respect to g_0 and g_1 at $\langle n \rangle = 1/2$ and $\langle n \rangle = 1/4$ for U = 0, 2 and 10. figures clearly show the metal-insulator transitions. Here we can have two types of insulating phases. Based on the values of U, g_0 and g_1 , we can have a SDW insulator or a CDW insulator. Fig. 10(a) describes the nature of PCC in the $(g_0 - g_1)$ – plane for U = 0 at $\langle n \rangle = 1/4$. The system is clearly metallic at low values of g_0 and g_1 , and it finally becomes insulating as g_0 and g_1 increase. This insulating GS would be a CDW state and contain local bipolarons due to the strong e-p interactions. In Figs. 10(b) and 10(c), PCC is plotted in the $(g_0 - g_1)$ plane at $\langle n \rangle = 1/4$ for U = 2 and U = 10respectively. These figures clearly show that in nonhalf-filled cases, metallic states can exist at small values of g_0 and g_1 even if U is large. The existence of this

metallicity is understandable because for < n > < 1/4, the probability for the system to have more empty sites is large which will certainly increase the mobility. The metal-insulator transition occurring because of the increase in the e-p coupling is obviously the Metal-CDW phase transition. The behaviour of PCC with respect to g_0 and g_1 is displayed in Fig. 10(d) at half filling for U = 0. The GS again shows a metallic behaviour at low values of g_0 and g_1 . As the values of g_0 and g_1 are increased, the system makes a transition into an insulating phase. However, unlike in



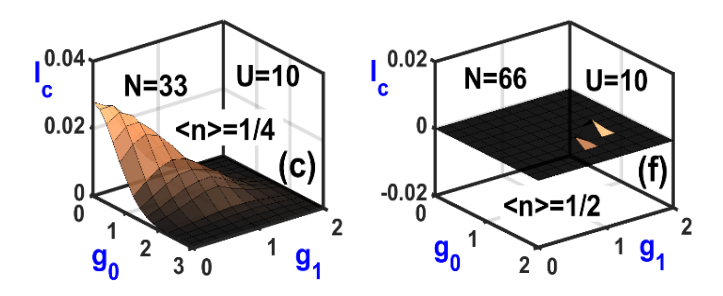
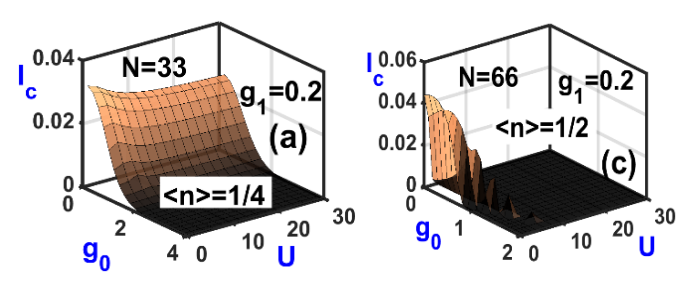


Fig. 10 I_c vs g_0 and g_1 for: (a) U=0, $\langle n \rangle = 1/4$; (b) U=2, $\langle n \rangle = 1/4$; (c) U=10, $\langle n \rangle = 1/4$; (d) U=0, $\langle n \rangle = 1/2$; (e) U=2, $\langle n \rangle = 1/2$; (f) U=10, $\langle n \rangle = 1/2$.

the non-half-filled case, the transition to the insulating phase of the system is much faster now. To be precise, compared to the case of $\langle n \rangle = 1/4$, the system now makes a transition to the insulating phase at lower values of e-p coupling constants. The incorporation of e-e interaction changes the situation significantly. In Fig. 10(e), we show how PCC varies with g_0 and g_1 for U = 2 at $\langle n \rangle = 1/2$. The system now behaves as an insulator even at low values of g_0 and g_1 . This insulating state clearly corresponds to an SDW state as U is finite and positive and the e-pinteractions are completely absent. This corresponds Mott insulating phase which is the antiferromagnetic phase arising due to Coulomb correlation. It is observed that as g_0 and g_1 are made very large, PCC drops to zero and hence the system

then again behaves as an insulator. In this case, U_{eff} becomes negative due to large values of g_0 and g_1 and so the effective force between electrons becomes attractive. Consequently, the system becomes unstable against Peierls distortion, and as a result bipolarons are formed and the system goes into a CDW insulator. However, for intermediate values of g_0 and g_1 , the system prefers to be in a metallic phase. Thus, one should observe a metallic phase flanked by two insulating phases for moderate values of g_0 and g_1 . One would thus expect the system to exhibit an SDW-Metal-CDW transition at half filling, in a certain window of U, g_0 and g_1 , if the e-p couplings are increased. As shown in Fig. 10(f), there is a complete suppression in the value of PCC at large value of U for all values of g_0 and g_1 and as a result the system behaves as an insulator for all values of g_0 and g_1 . Although the transition region is a bit unclear now, it seems that in this case, the system makes a direct transition from SDW phase to the CDW phase as the e-p couplings become stronger.



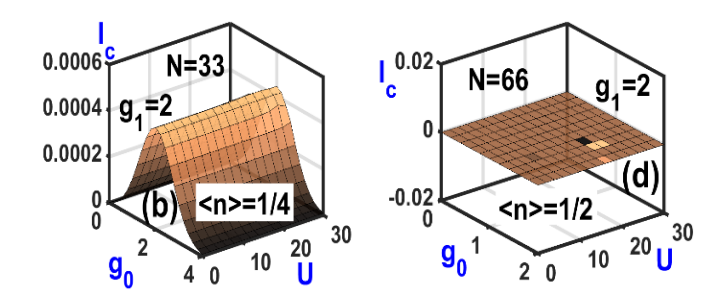


Fig. 11 I_c vs g_0 and U for : (a) $g_1=0.2$, $\langle n\rangle=1/4$; (b) $g_1=2$, $\langle n\rangle=1/4$; (c) $g_1=0.2$, $\langle n\rangle=1/2$; (d) $g_1=2$, $\langle n\rangle=1/2$

To examine the phase transition behaviour more critically, we plot PCC versus U and g_0 for $g_1 = 0.2$ and $g_1 = 2$ at < n > = 1/2 and < n > = 1/4 in Fig. 11. Fig. 11(a) is plotted for $g_1 = 0.2$ and $\langle n \rangle$ = 1/4. It can be clearly noticed from this figure that when the values of g_0 and U are small, GS of the system is of course metallic. Furthermore, the system continues to be in the metallic phase even at large U at low g_0 . This happens probably because of the availability of many sites for occupation in the case of less-than half-filling. So, at small g_0 , as GS of the system is essentially determined by the e-p interaction, even a large Coulomb interaction cannot push it to the insulating phase. However, if g_0 is increased, the system can be driven to an insulating phase which at low U would be a CDW phase owing to bipolaron formation. Similarly, if U is increased, the system can

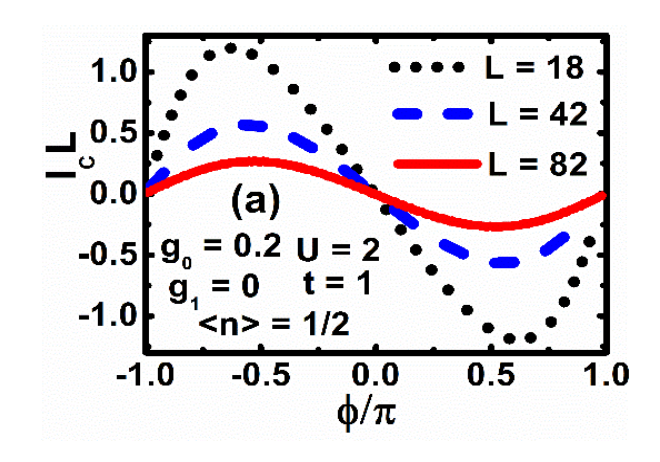
again be driven into an insulating phase, though this insulating phase would be an SDW phase. So, the present system can exhibit a Metal-CDW transition at small U and a Metal-SDW transition at large U. On the other hand, at large g_0 , there exists a critical value of Uat which the system goes directly from an insulating CDW phase to the insulating SDW phase. In Fig. 11(b), we consider the behavior of PCC with respect to U and g_0 for $g_1 = 2$. In a certain window of (U, Y_0) g_0) – values, the system shows a metallic behaviour. As g_1 is increased, we observe suppression in the magnitude of PCC. Whether the insulating phase will correspond to SDW or CDW depends on the relative values of U and g_0 . In Fig. 11(c), we show the behaviour of PCC with respect to U and g_0 for $g_1 =$ 0.2 at $\langle n \rangle = 1/2$. The system now shows a conducting behaviour at low values of U and g_0 . At small g_0 , the system however goes from a metallic phase to an insulating state at some critical U. This insulating phase is an SDW state. Similarly, at small U, the system undergoes a metal-insulator transition at some critical g_0 . This insulating state is a CDW state. In Fig. 11(d), we plot PCC with respect to U and g_0 with $g_1 = 2$ at $\langle n \rangle = 1/2$. In this situation, the system remains in the insulating phase for all U and g_0 . Here, too, the system may undergo a CDW-SDW transition, but the transition boundary looks obscure. We have also examined the nature of variation of PCC

with respect to U and g_1 for $g_1 = 0.2$ and $g_1 = 2$ at < n > = 1/2 and < n > = 1/4. (Figures have not been shown here). The behaviour is more or less similar to that shown in Fig. 11.

(e) Size dependence of PCC

Fig. 12 shows the behaviour of I_cL (i.e., PCC scaled by the system size L) with respect to the flux ϕ for a few L – values. The figure demonstrates that periodicity of I_c is independent of L at < n > = 1/2, while for $< n > \neq 1/2$, it increases with L.

In Fig. 13 (a) we plot $ln(I_cL)$ with L for a few values of U and e-p interactions at < n > = 1/2. One may notice that $ln(I_cL)$ varies more or less linearly with (-L) i.e. $ln(I_cL)$ decreases linearly with increasing L. Fig. 13 (b) shows the behaviour of $ln(I_c)$ with respect to ln(L) for < n > = 2/5 which is a non-half-filled case. We find that $ln(I_c)$ exhibits a linear behaviour with ln(L) and furthermore $ln(I_c)$ turns out be essentially independent of of U, g_0 and g_1 .



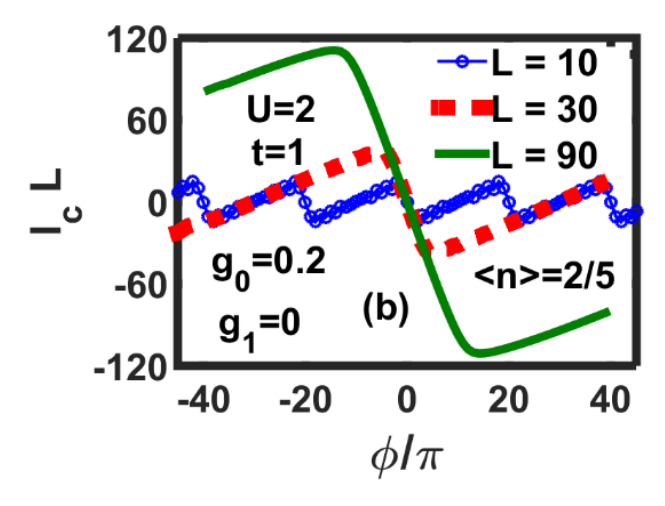


Fig. 12 I_c vs ϕ for different values of L with $g_0 = 0.2$, $g_1 = 0$, U = 2 for (a) < n > = 1/2; for (b) < n > = 2/5.

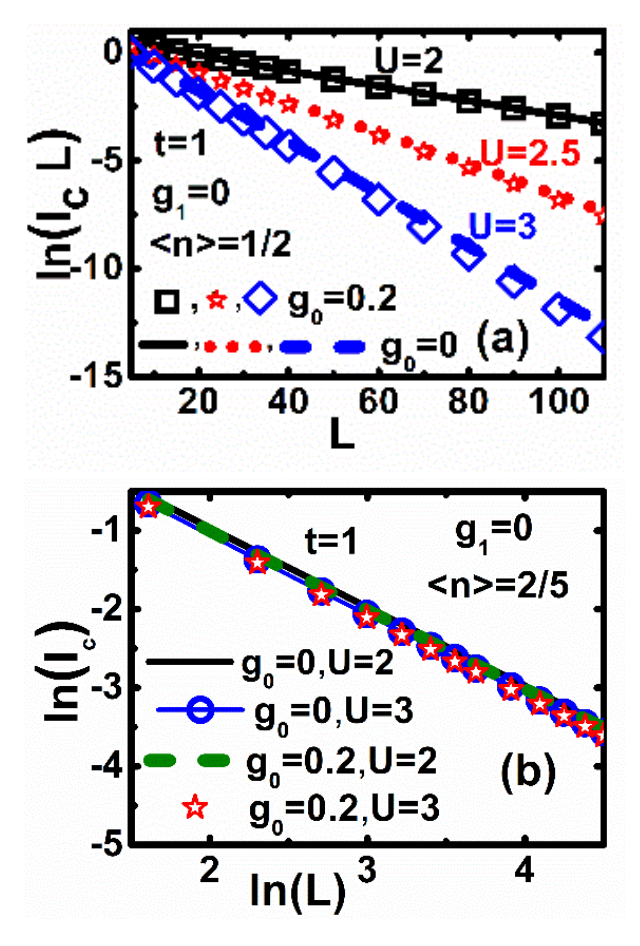


Fig. 13 $\ln(I_c L)$ vs L for $\langle n \rangle = 1/2$ and different values of U: (a) $g_1 = 0$, $g_0 = 0$, 0.2; (b) $g_0 = 0$, $g_1 = 0$, 0.2. $\ln(I_c L)$ vs $\ln L$ for $\langle n \rangle = 2/5$ and different values of U: (b) $g_1 = 0$, $g_0 = 0$, 0.2.

3.4.3. Persistent spin current (PSC)

(a) Flux-dependence of PSC

In Fig. 14, we plot PSC (I_s) with respect to flux ϕ for a few values of g_0 at < n > = 1/2. We find that the spin current is periodic but does not have the sinusoidal nature.

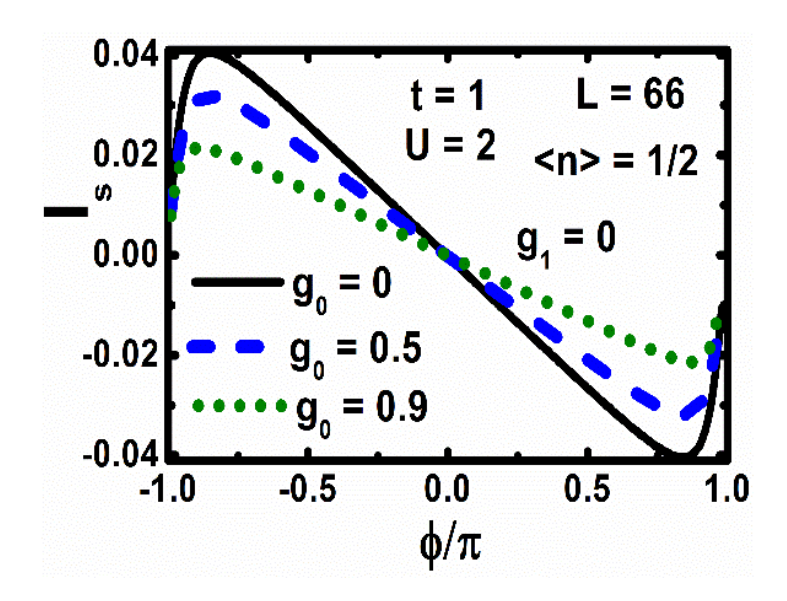


Fig. 14 I_s vs ϕ for different values of g_0 .

(b) PSC and Coulomb Correlation

In Fig. 15, we study how PSC behaves with respect to U for a few values of g_0 at < n > = 1/2 and also at $< n > \neq 1/2$. The behaviour is found to be, in general, concave from above and both Coulomb correlation and e-p interaction are found to suppress I_s .

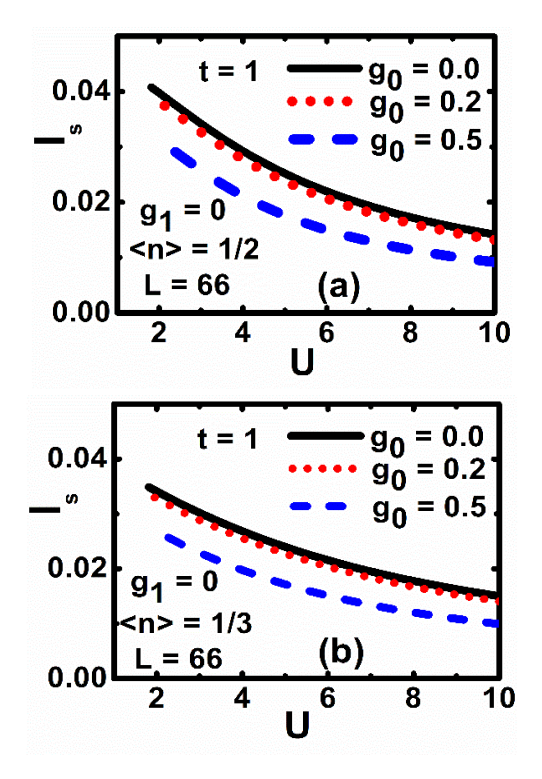
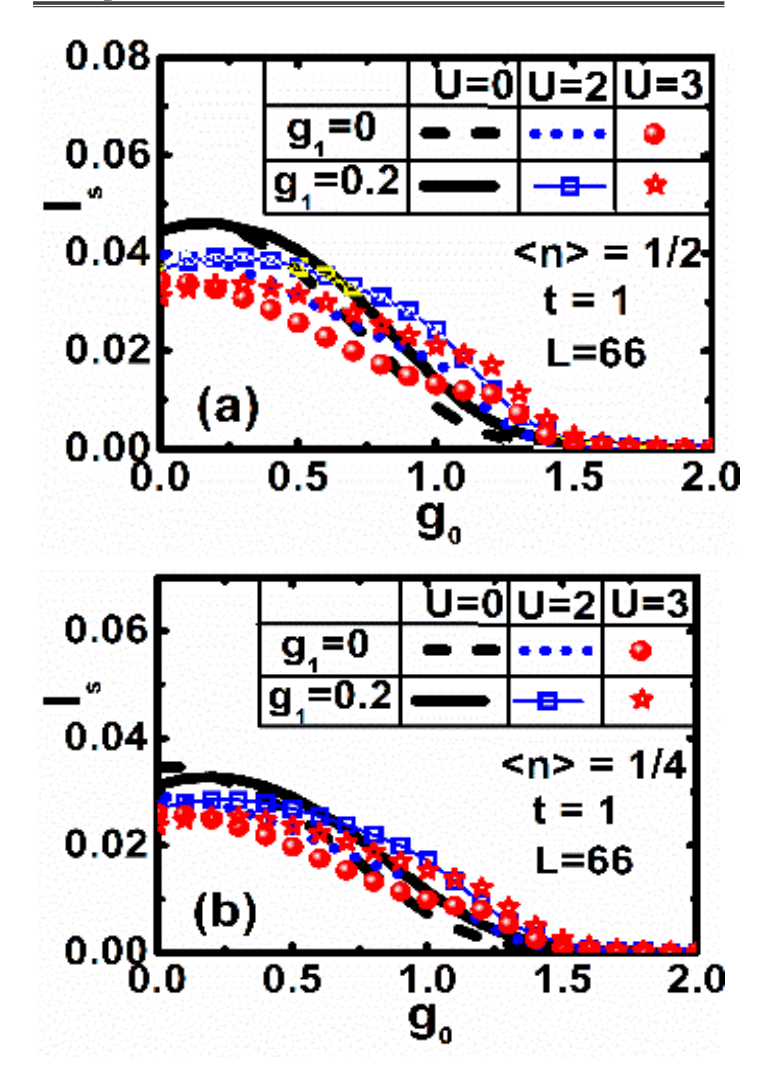


Fig. 15 I_c vs U for different values of g_0 and (a) < n > = 1/2; (b) < n > = 1/3

Chapter 3: Persistent Currents in the 1D Holstein....



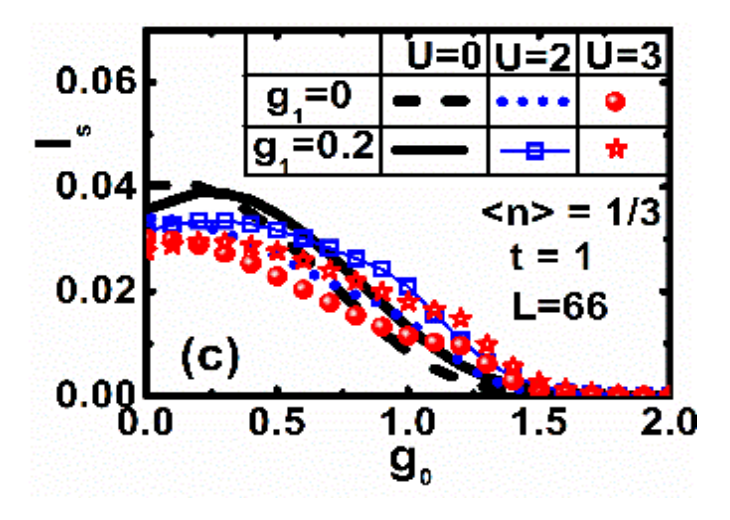


Fig. 16 PSC I_s as a function of g_0 for different values of U and g_1 with L=66 at (a) half filling (< n>=1/2); (b) < n>=1/4; (c) < n>=1/3

(c) PSC and *e-p* interaction

In Fig. 16, we display the behavior of PSC (I_s) with respect to g_0 for different combinations of the U and g_1 . Fig. 16(a) provides results for < n > = 1/2 and Figs. 16(b, c) show the results for $< n > \neq 1/2$. In all cases, PSC reduces with increasing g_0 .

(d)Size dependence of PSC

Fig. 17 describes the behavior of PSC with respect to flux for a few values of L. It is evident from the figure as L decreases, I_s undergoes an enhancement. The reason is understandable because the persistent current is a quantum phenomenon which arises at a small length scale where quantum effects become more significant.

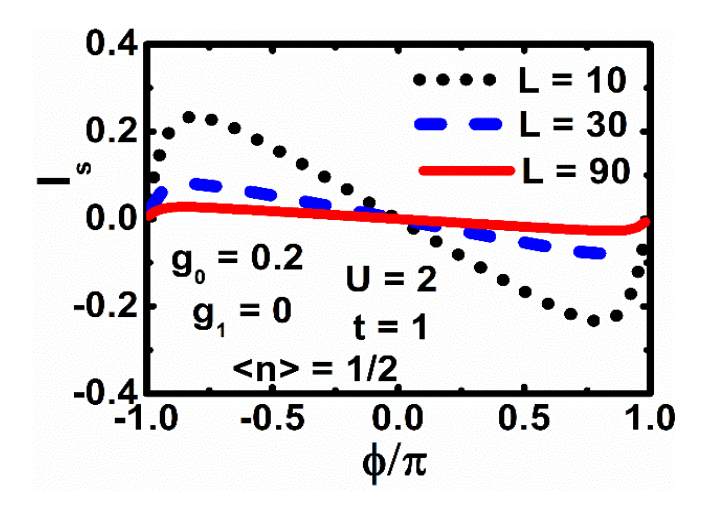


Fig. 17 I_c vs ϕ for different values of L $g_0 = 0.2$, $g_1 = 0$ at < n > = 1/2.

3.5 Summary and Conclusion

In conclusion, the Holstein-Hubbard model has been considered for a finite QR with the Aharonov-Bohm flux. The conventional canonical Lang-Firsov transformation approach is utilized to treat the e-p interaction and subsequently the Bethe Ansatz technique is employed to deal with the effective electronic Hamiltonian. This provides a set of coupled transcendental equations which are solved by using an iterative computational technique for the half-filled and a few non-half-filled cases to obtain the GS energy. The persistent charge current and persistent spin current are then computed by differentiating the GS energy with respect to the AB flux and investigated with respect to the system parameters such as the onsite e-e strength U, onsite e-p strength g_0 and the NN *e-p* interaction strength g_1 .

We observe that the GS obtained by the exact Bethe ansatz technique is higher than that estimated by the mean-field approximation. Also the peaks are much sharper now. In both the half-filled and away from half-filled cases, the GS energy is periodic in the magnetic flux, though in the non-half-filled case, the periodicity is, in addition, dependent on the ring size. Again, in the half-filled case, low values of U are

favourable for GS while large values of *U* are more conducive for GS for the non-half-filled cases.

In the case of half-filling, the periodicity of GS with respect to the flux leads to a sinusoidal variation of PCC with the flux. As the *e-p* coupling is raised, though the behaviour of PCC no longer remains sinusoidal, it still continues to be periodic. The current now undergoes an increase. This increase in current my happen on account of the motion of correlated bipolarons. In the non-half-filled cases, PCC again shows a periodic variation with the flux, but the periodicity scales linearly with the system size. PSC is also periodic but non-sinusoidal. The PCC versus U – data for both the half-filled and non-half-filled cases can be fitted to two different analytical expressions if the *e-p* interaction is absent. The decrease in QR size is found to enhance both PCC and PSC. This is an understandable result because the persistent currents are of quantum mechanical origin and are therefore expected to occur when the length scales are sufficiently small. It is also observed that both e-e and ep interactions suppress the persistent currents for the half-filled and non-half-filled cases. It is further shown that in the weak e-p coupling regime, the system likes to be in a metallic phase at away from half filling, while a sufficient increase in the e-p coupling may drive the system to an insulating state. This metal-insulator transition may be considered as a Metal-CDW transition which is little affected by the electron correlation. A half-filled system is however associated with interesting quantum phase transitions. While in the absence of electron correlation, as the *e-p* interaction strength is increased, a Metal-CDW phase transition occurs, in the presence of both *e-e* and *e-p* interactions, a CDW-Metal-SDW transition takes place for certain ranges of the parameter values. A substantially large value of *e-e* coupling strength is unfavourable for the metallic phase because it drives the system to the SDW state.

References

- L. P. Levy, G. Dolan, J. Dunsmuir, and H. Bouchiat, *Phys. Rev. Lett.* 64, no. 17, pp. 2074-2077, (1990).
- V. Chandrasekhar, R. A. Webb, M. J. Brady, M. B. Ketchen, W. J. Gallagher, and A. Kleinsasser, *Phys. Rev. Lett.* 67, no. 25, pp. 3578-3581, (1991).
- 3. D. Mailly, C. Chapelier and A. Benoit, *Phys.* Rev. Lett. **70**, no. 13, pp. 2020-2023, (1993).
- B. Reulet, M. Ramin, H. Bouchiat and D. Mailly, *Phys. Rev. Lett.* 75, no. 1, pp. 124-127, (1995).

Chapter 3: Persistent Currents in the 1D Holstein....

- E. M. Q. Jariwala, P. Mohanty, M. B. Ketchen and R. A. Webb, *Phys. Rev. Lett.* 86, no. 8, pp. 1594-1597, (2001).
- R. Deblock, R. Bel, B. Reulet, H. Bouchiat and D. Mailly, *Phys. Rev. Lett.* 89, no. 20, pp. 206803 (1-4), (2002).
- H. Bluhm et al., *Phys. Rev. Lett.* **102**, pp. 136802 (1-4), (2009).
- A.C. Bleszynski-Jayich, et al., Science 326, pp. 272-276 (2009); N. O. Birge, Science. 326, pp. 244-245, (2009).
- 9. G.M. Souche, et al., *Phys. Rev. B.* **87**, pp. 115120 (1-6), (2013).
- 10. M.A. Castellanos-Beltran et al., *Phys. Rev. Lett.* **110**, pp. 156801 (1-5), (2013).
- A. Moskova, M. Mosko, J. Tobik, *Phys. Status Solidi B* 250, no. 1. pp. 147-159, (2013).
- 12. R. Landauer and M. B"uttiker, *Phys. Rev. Lett.* **54**, no. 18, pp. 2049-2052, (1985).

- H. F. Cheung, Y. Gefen, E. K. Riedel and W. H. Shih, *Phys. Rev. B* 37, no. 11, pp. 6050-6062 (1988).
- 14. B. L. Altshuler, Y. Gefen and Y. Imry, *Phys. Rev. Lett.* **66**, no. 1, pp. 88-91 (1991).
- 15. F. von Oppen and E. K. Riedel *Phys. Rev. Lett.* **66**, no. 1, pp. 84-87, (1991).
- 16. A. Schmid, *Phys. Rev. Lett.* **66**, no. 1, pp. 80-83, (1991).
- 17. M. Abraham and R. Berkovits, *Phys. Rev. Lett.* **70**, no. 10, pp. 1509-1512, (1993).
- 18. O.V. Kibis, O. Kyriienko, I.A. Shelykh, *Phys. Rev. B* **87**, pp. 245437 (1-6), (2013).
- 19. B.B. Wei, S.J. Gu, H.Q. Lin, *J. Phys.: Cond. Matt.* **20**, pp. 395209 (1-8), (2008).
- 20. I.V. Sankar, P.J. Monisha, S. Sil and Ashok Chatterjee, *Physica E.* **73**, pp.175-180, (2015).

Chapter 4

Summary and Conclusions

In this concluding chapter, we present the summary of the present thesis.

In Chapter 1, we have presented some of the basic concepts and the models that have been used in the works described in the thesis. We have started with the Tight-binding model of the band theory and presented the energy dispersion provided by this model because in this thesis, we are interested in the narrow-band systems with localized states. Since the celebrated Hubbard model is one of the most suitable models to study the role of e-e interaction in strongly correlated systems, we have then presented a brief description of this model. Next, we have discussed phonons and the polarons and bipolarons and described briefly the physics of these quasi-particles and introduced the Holstein model. Finally, we have combined the Holstein and the Hubbard models and presented the Holstein-Hubbard model which can describe the physics of a correlated electron system with electronphonon interaction. Subsequently, we have discussed the ground state phases namely, the SDW and CDW

phases provided by the Holstein-Hubbard model and the possible phase transitions that are possible within the framework of this model. Next, we have discussed the motivation for studying the GS phases of the Holstein-Hubbard model in this thesis. Finally, we have given a brief introduction to Persistent current in a mesoscopic ring and described our motivation to study this phenomenon.

One of our main aims in this thesis has been to explore the effect of the Gaussian phonon anharmonicity on the intermediate metallic phase that may exist at the crossover region of the CDW-SDW phases in a 1D Holstein-Hubbard system. In Chapter 2, we have presented our recent investigation on this issue. Here we have considered a better variational phonon state than in [1] to obtain an effective Hubbard model which has been solved exactly by the Bethe ansatz technique to obtain the GS energy. We have calculated the local spin moment and considered the Mott criterion. We have also calculated the double occupancy and the single-site entanglement entropy for half and non-half band fillings. We first observe that though at small Coulomb correlation strength, the phonon anharmonicity does not have much effect on the GS energy, at large Coulomb interaction, anharmonicity does enhance the GS energy. We find that in the presence of anharmonicity, the Holstein band reduction factor diminishes rapidly with increasing e-p coupling. We also find that as the e-p coupling is increased, the system undergoes a transition from the polaronic SDW GS to the bipolaronic CDW GS state through an intermediate metallic phase. It is shown that anharmonicity widens the intermediate metallic phase. Also the present calculation provides a broader metallic phase than the one predicted by the previous calculation [2]. It has been further shown that the broadening of the width of the metallic phase is more if the anharmonicity lies in a certain window. The calculation of the average spin moment per site, the double occupancy and the entanglement entropy also provide the evidence that an intervening metallic phase exists at the CDW-SDW transition region. It is important to note that the present improved variational calculation suggests a wider metallic phase which reinforces the prediction that an intermediate metallic phase exists at the CDW-SDW crossover region.

In Chapter 3 we have presented our calculation of the persistent charge and spin currents in a quantum ring threaded with magnetic flux in the presence of *e-e* and *e-p* interactions. We have used the Holstein-Hubbard model to study the effect of the interplay of the *e-e* and *e-p* interactions. The *e-p* interaction has been treated using the standard Lang-Firsov method and the effective renormalized electronic system has been solved using the Bethe-ansatz technique. It has been shown that the Bethe ansatz provides a larger GS

energy than the mean-field approximation. For the half-filled case, GS corresponds to low e-e interaction strength while for the case of away from half filling, GS corresponds to larger values of the correlation strength. The GS energy and the persistent currents are periodic in the magnetic flux both in the half-filling and non-half-filling cases. A decrease in the quantum ring size is found to increase the persistent currents. This is precisely the quantum effect. Both for halffilling and non-half-filling cases, the persistent currents are suppressed by the e-e and e-p interactions. Interestingly, it is found that in the absence of electron correlation, as the e-p coupling is increased, a Metal-CDW phase transition occurs in the Holstein-Hubbard ring, while in the presence of both e-e and e-p interactions, a CDW-Metal-SDW transition takes place for certain ranges of the parameter values. However, a substantially large value of e-e coupling strength turns out to be unfavourable for the metallic phase because it drives the system to the SDW insulating state.

Before we end, we would like to mention that the results presented in the present thesis may be improved by choosing more improved phonon states.

References

- 1. Y. Takada and A. Chatterjee, *Phys. Rev. B.* **67**, pp. 081102 (1-4), (2003).
- 2. A. Chatterjee and Y. Takada, *J. Phys. Soc. Jap.* **73**, no. 4, pp. 964-969, (2004).

List of Publications

Peer reviewed journals

- Ch. Uma Lavanya, I.V. Sankar and Ashok Chatterjee, Metallicity in a Holstein-Hubbard Chain at half filling with Gaussian Anharmonicity, Scientific Reports 7 3774 (2017).
- Ch. Uma Lavanya and Ashok Chatterjee, Persistent and Spin Currents in the 1D Holstein-Hubbard ring at half filling and at away from halffilling by Bethe-ansatz approach, *Physica E* 126 114500 (2021).

Conference Proceedings

- Ch. Uma Lavanya and Ashok Chatterjee, The Holstein-Hubbard Model with Gaussian Anharmonicity in one-Dimension at Half-filling, AIP Conference Proceedings 1728 020477 (2016).
- Ch. Uma Lavanya and Ashok Chatterjee, Metallicity of the anharmonic Holstein-Hubbard Model in the adiabatic regime, AIP Conference Proceedings 1942 090003 (2018).

Phase Transitions in One-Dimensional Holstein-Hubbard Chain and Ring

by Chintapanti Uma Lavanya

Submission date: 08-Nov-2021 02:35PM (UTC+0530)

Submission ID: 1696518392

File name: Ph.D._Thesis_12PHPH08_by_Ch._Uma_Lavanya.pdf (2.81M)

Word count: 15698 Character count: 73429 UNIVERSITY OF HYDERABAD Central University P.Q. HYDERABAD-500 046

Phase Transitions in One-Dimensional Holstein-Hubbard Chain and Ring

ORIGINALITY REPORT

17%

6%

17%

0%

SIMILARITY INDEX

INTERNET SOURCES

PUBLICATIONS

STUDENT PAPERS

PRIMARY SOURCES

Ch. Uma Lavanya, Ashok Chatterjee.
"Persistent Charge and Spin Currents in the
1D Holstein-Hubbard ring at half filling and
at away from half filling by Bethe-ansatz
approach", Physica E: Low-dimensional
Systems and Nanostructures, 2020

8%

Prof. ASHOK CHATTERJEE SCHOOL OF PHYSICS UNIVERSITY OF HYDERABAD HYDERABAD - 500 046, INDIA

Publication

www.nature.com

Internet Source

3%

mafiadoc.com

Internet Source

1 %

Ch. Uma Lavanya, I. V. Sankar, Ashok Chatterjee. "Metallicity in a Holstein-Hubbard Chain at Half Filling with Gaussian Anharmonicity", Scientific Reports, 2017



Prof. ASHOK CHATTERJEE SCHOOL OF PHYSICS UNIVERSITY OF HYDERABAD HYDERABAD - 500 046, INDIA

%

www.ncbi.nlm.nih.gov

Internet Source

Ch Uma Lavanya, Ashok Chatterjee.

"Persistent charge and spin currents in the
1D Holstein-Hubbard ring at half filling and

Production Chairersee SCHOOL OF PHYSICS UNIVERSITION HYDERABAD HYDERABAD - 500 MG INDIA

The total similarity index is 17% out of which is from her own fullienters. So which is from her own fullienters. So which is which is within the se effective similarity onder is 7% which is within the last of 10% Creek.

at away from half filling by Bethe-ansatz approach", Physica E: Low-dimensional Systems and Nanostructures, 2021

Publication

Md. Zahid Malik, Ashok Chatterjee. "An Intervening metallic phase at the CDW-SDW transition region in the one-dimensional Holstein-Hubbard model at half filling: A Semi-Exact solution", Journal of Physics Communications, 2020

<1%

- Publication
- I.V. Sankar, P J Monisha, Shreekantha Sil, Ashok Chatterjee. "Persistent current and the existence of a metallic phase flanked by two insulating phases in a quantum ring with both electron–electron and electron– phonon interactions", Physica E: Lowdimensional Systems and Nanostructures, 2015

<1%

- Publication
- Debika Debnath, M. Zahid Malik, Ashok Chatterjee. "A semi exact solution for a metallic phase in a Holstein-Hubbard chain at half filling with Gaussian anharmonic phonons", Scientific Reports, 2021

<1%

I.V. Sankar, Ashok Chatterjee. "Quantum phase transition in a one-dimensional Holstein-Hubbard model at half-filling in the thermodynamic limit: A quantum

<1%

entanglement approach", Physica B: Condensed Matter, 2016

Publication

Manasa Kalla, Narasimha Raju Chebrolu, Ashok Chatterjee. "Quantum transport in a single molecular transistor at finite temperature", Scientific Reports, 2021 <1%

Publication

P. Quémerais. "Theory of charge density wave depinning by electromechanical effect", EPL (Europhysics Letters), 2017

<1%

Publication

Masatoshi Imada. "Metal-insulator transitions", Reviews of Modern Physics, 10/1998

<1%

Publication

Ashok Chatterjee. "Existence of an Intermediate Metallic Phase at the SDW-CDW Crossover Region in the One-Dimensional Holstein-Hubbard Model at Half-Filling", Advances in Condensed Matter Physics, 2010

<1%

Bo-Bo Wei, Shi-Jian Gu, Hai-Qing Lin.
"Persistent currents in the one-dimensional mesoscopic Hubbard ring", Journal of Physics: Condensed Matter, 2008

Publication

<1%

"Strongly Correlated Systems", Springer Science and Business Media LLC, 2012

<1%

	. abitedioi:	
17	lup.lub.lu.se Internet Source	<1%
18	Kulic, M.L "Interplay of electron-phonon interaction and strong correlations: the possible way to high-temperature superconductivity", Physics Reports, 200011	<1%
19	P. J. Monisha, I. V. Sankar, Shreekantha Sil, Ashok Chatterjee. "Persistent current in a correlated quantum ring with electron- phonon interaction in the presence of Rashba interaction and Aharonov-Bohm flux", Scientific Reports, 2016 Publication	<1%
20	Anastassakis, E M, and J D Joannopoulous. "The Physics of Semiconductors: 20th International Conference", The Physics of Semiconductors, 1990. Publication	<1%
21	Hitoshi Nitta, Masato Suzuki, Takeshi Iida. "Adiabatic nature of hole-doped states in strongly coupled electron-phonon systems", Physical Review B, 2000 Publication	<1%
22	Miodrag L. Kulić. "Interplay of electron- phonon interaction and strong correlations: the possible way to high-temperature superconductivity", Physics Reports, 2000 Publication	<1%

23

M Zahid Malik, Ashok Chatterjee. "An intervening metallic phase at the CDW-SDW transition region in the one-dimensional Holstein-Hubbard model at half filling: a semi-exact solution", Journal of Physics Communications, 2020

Publication

Exclude quotes On Exclude bibliography On

Exclude matches

< 14 words

<1%